RECENT RESEARCH ACTIVITIES

Start-up Experiment for Biochemical/Biophysical Study of Cellulose Biosynthesis

(Laboratory of Biomass Morphogenesis and Information, RISH, Kyoto University)

Tomoya Imai

Living organisms produce 100 billion tons of cellulose each year. Such massive cellulose production on earth means that the ability to synthesize cellulose has been beneficial to the organisms that acquired this ability through evolution, and that it has been "SUSTAINABLE" material in biosphere. The most striking example will be seen in the plant cell walls, in which cellulose plays an important role to support a tall tree such as 100-m. This is because cellulose has strong mechanical strength and biological resistance by virtue of its high crystalline fibrous structure with hydrogen bonding network, microfibril.

In spite of such ubiquitousness on earth, the enzymatic mechanism of cellulose biosynthesis is not well understood since most of researches focus on the molecular and cellular biological aspect of cellulose biosynthesis. This is probably because cellulose synthase is membrane protein and hetero-subunit complex, and extremely difficult to analyze the enzyme itself. Thus now, biochemical/biophysical analyses are absolutely demanded for understanding how cellulose microfibril is synthesized by cellulose synthase in lipid bilayer of cell membrane. For this purpose, cellulose synthase and its enzymatic activity must be directly analyzed in more detailed. I am challenging it using a cellulose-producing bacterium *Gluconacetobacter xylinus*. This is only one organism from which cellulose-synthesizing activity can be extracted without enzymatic contamination, allowing the direct analysis of cellulose synthase.

Enzyme assay paves the way for clarifying biochemical/biophysical aspects of cellulose biosynthesis

Previously reported protocol to extract the activity [1] uses PEG (polyethylene glycol) in buffer, which is unfavorable for many of biochemical analyses. Furthermore there is room for testing detergents to solubilize the activity from cell membrane, because many new detergents have been introduced since the previous protocol was often used in 1980's. Then two points are considered for establishing a new protocol: (i) removing PEG from buffer and (ii) solubilization by mild detergent. A new protocol is thus successfully established with no PEG and solubilization by detergent that has not been tested, like alkylmaltoside [2].

The access to enzymatic assay by this protocol allows biochemical analyses to be carried out (Figure 1). As well, the formation of cellulose microfibril will be investigated in a view of biophysics. These together will lead us to comprehensive understanding of cellulose biosynthesis.

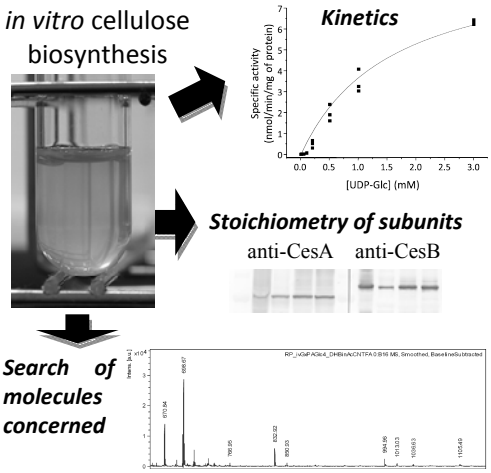

Figure 1. Established *in vitro* cellulose biosynthesis and the researches derived from it. These are actually in progress.

Acknowledgements

The author appreciates Mr. Akira Hashimoto and Kenji Shimono for their works during their master course in Graduate School of Agriculture, Kyoto University.

References

[1] Aloni, Y., Cohen, R., Benziman, M., Delmer, D. "Solubilization of the UDP-glucose: 1,4-β-glucan-4-β-D-glucosyltransferase (cellulose synthase) from *Acetobacter xylinum*. A comparison of regulatory properties with those of the membrane-bound form of the enzyme," *J.Biol.Chem.* **258**, 4419-4423, 1983.

[2] Hashimoto, A., Shimono, K., Horikawa, Y., Ichikawa, T., Wada, M., Imai, T., Sugiyama, J. "Extraction of cellulose-synthesizing activity of *Gluconacetobacter xylinus* by alkylmaltoside." *Carbohydr.Res.* **346**, 2760-2768, 2011.

RECENT RESEARCH ACTIVITIES

Novel unsaturated ceriporic acids involved in ligninolytic lipid peroxidation produced by *Ceriporiopsis subvermispora*

(Laboratory of Biomass Conversion, RISH, Kyoto University)

Hiroshi Nishimura and Takashi Watanabe

Photosynthetic plants are the principal solar energy converter sustaining life on Earth. White-rot fungi play an important role in the carbon cycle in earth's ecosystems because they efficiently degrade plant cell walls that are impregnated with lignin. In lignin biodegradation, the cleavage of recalcitrant non-phenolic substructures has been regarded as an essential prerequisite for the efficient degradability of lignin by enzymatic reactions. For instance, lignin peroxidase (LiP) has been proposed to drive lignin degradation because of its high oxidation potential, which is sufficiently high to degrade the non-phenolic lignin substructure. However, the selective white-rot fungus *Ceriporiopsis subvermispora* degrades the recalcitrant non-phenolic lignin substructure without expressing detectable LiP. Lipid peroxidation catalyzed by manganese peroxidase (MnP) was proposed as a mechanism for the lignin biodegradation, because the reaction decomposed the non-phenolic lignin dimer model compound. Accumulation profiles of fatty acids, lipid hydroperoxides, aldehydes, and titers of MnP in wood cultures of *C. subvermispora* supported the fact that lipid peroxidation by MnP is involved in the incipient stage of wood decay by the fungus. In this study, new ceriporic acids—alkadienyl, alkenyl and epoxy itaconic acids (ceriporic acid G, H and epoxy ceriporic acid)—were isolated from the cultures of the selective lignin-degrading fungus *C. subvermispora*.[1–3] The new metabolites ceriporic acid G and H were synthesized by a cross-aldol condensation and a Grignard reaction, respectively. Ceriporic acid G triggered the MnP-catalyzed lipid peroxidation and decomposed a recalcitrant non-phenolic lignin substructure model compound (Figure 1). Except for simple fatty acids, this is the first report of a fungal metabolite that induced ligninolytic lipid peroxidation.

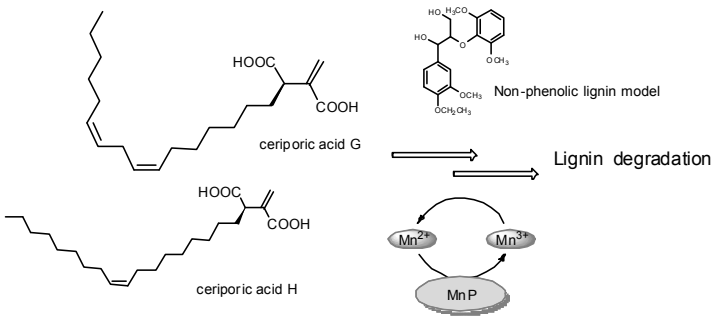

Figure 1. MnP and the novel ceriporic acids initiate lipid peroxidation to degrade a recalcitrant non-phenolic lignin substructure model compound.

References

[1] Nishimura, H., Y. Setogawa, T. Watanabe, Y. Honda and T. Watanabe: Epoxy ceriporic acid produced by selective lignin-degrading fungus *Ceriporiopsis subvermispora*, Chem. Phys. Lipids, 164, 707-712 (2011).

[2] Nishimura, H., K. Murayama, T. Watanabe, Y. Honda and T. Watanabe: Diverse rare lipid-related metabolites including ω-7 and ω-9 alkenylitaconic acids (ceriporic acids) secreted by a selective white rot fungus, *Ceriporiopsis subvermispora*, Chem. Phys. Lipids, 165, 97-104 (2012).

[3] Nishimura, H., M. Sasaki, H. Seike, M. Nakamura and T. Watanabe: Alkadienyl and alkenyl itaconic acids (ceriporic acids G and H) from the selective white fungus *Ceriporiopsis subvermispora*: A new class of metabolites initiating ligninolytic lipid peroxidation, Org. Biomol. Chem., 10, 6432-6442 (2012).

RECENT RESEARCH ACTIVITIES

Development of high-throughput characterization of lignocelluloses and the analysis of lignocelluloses from *Jatropha curcas* (Laboratory of Metabolic Science of Forest Plants and Microorganisms, RISH, Kyoto University)

Toshiaki Umezawa and Shiro Suzuki

It is becoming more important to establish a sustainable society, which depends on renewable resources. Wood biomass is the most abundant renewable resource on the earth, and therefore, the better utilization and efficient production of wood biomass are the key factors to establish a sustainable society. In this context, our laboratory is involved in analyzing metabolic functions of forest plants from a wide variety of aspects, including organic chemistry, biochemistry, molecular biology, and metabolomics, aiming at the elucidation of mechanisms of wood formation of biomass plants and their biotechnological application. Here we describe some of the recent research topics of our laboratory.

1. High-throughput lignin characterization and determination and saccharification efficiency

In molecular breeding of wood biomass plants, straight-forward, high-throughput, and microscale characterization of wood biomass components is important to select the best recombinant lines at the stage of juvenile plantlets. Because lignin is one of the major components in wood biomass, its biosynthesis is one of the major targets in molecular breeding of wood biomass plants. However, the conventional methods for lignin analysis are low-throughput and employ complicate experimental procedures. We have already modified the thioglycolic acid lignin determination and nitrobenzene oxidation method suitable for large number and small quantity of samples. We recently modified the thioacidolysis for rapid and microscaled analysis [1]. In addition, using near-infrared spectroscopy analysis, we established the rapid quantification system of lignin and starch contents and saccharification efficiency [2]. Using the analytical methods, we are selecting the rice plants to enable the efficient conversion of wood biomass to energy.

2. Analysis of lignocelluloses from *Jatropha curcas*

Jatropha curcas is one of promising oil producing plants because the plant produces large amounts of oil and shows an excellent adaptation capacity to a large variety of soil and climate conditions. *J. curcas* trees are trimmed to ca. 2 m in height to facilitate the harvesting of the fruits. As a result, *J. curcas* oil production is accompanied by the concomitant production of 10 ton ha^{-1} $year^{-1}$ of branches, which are discarded without utilization. The yield of the woody branches is almost similar to that of fast growing trees in temperate zone. Thus, the utilization of the trimmed braches is critically important for increasing the economical efficiency of *J. curcas* plantations. To exploit the branches as lignocellulosic raw materials for the production of pulp, paper, wooden board, and biofuels, it is necessary to characterize lignins in the branches. In this context, lignins of *J. curcas* organs were qualitatively and quantitatively characterized by thioglycolic acid, thioacidolysis, and nitrobenzene oxidation methods [3].

References

[1] M. Yamamura, T. Hattori, S. Suzuki, D. Shibata, T. Umezawa, “Microscale thioacidolysis method for the rapid analysis of β-O-4 substructures in lignin,” *Plant Biotechnology*, in press.

[2] T. Hattori, S. Murakami, M. Mukai, T. Yamada, H. Hirochika, M. Ike, K. Tokuyasu, S. Suzuki, M. Sakamoto, T. Umezawa, “Rapid analysis of transgenic rice straw using near-infrared spectroscopy,” *Plant Biotechnology*, in press.

[3] M. Yamamura, K. Akashi, A. Yokota, T. Hattori, S. Suzuki, D. Shibata, T. Umezawa, “Characterization of *Jatropha curcas* lignins,” *Plant Biotechnology*, in press.

RECENT RESEARCH ACTIVITIES

Metabolic engineering for prenylated flavonoids in transgenic plants using bacterial and plant prenyltransferases

(Laboratory of Plant Gene Expression, RISH, Kyoto University)

Akifumi Sugiyam, Kojiro Takanashi and Kazufumi Yazaki

Plants produce a large number of secondary metabolites that do not appear to be relevant for primary biological activity. Among these secondary metabolites, polyphenols are common to all plant species and are known as anti-oxidants and UV protectants. Polyphenols modified with prenyl residues have a variety of biological activities, such as anti-tumor, anti-bacterial, anti-virus, anti-oxidant, anti-tyrosinase and estrogenic. Although prenylated polyphenols are attractive natural products because of their various biological activities, their limited occurrence in plants as well as the difficulty of purification from complicated mixtures has limited the potential applications of these compounds for many years; therefore, metabolic engineering with prenyltransferase genes has been of particular interest. The identification of prenyltransferase genes from Streptomyces and *S. flavescens* enabled us to synthesize prenylated polyphenols via metabolic engineering. In this study, Streptomyces genes (*NphB*, *SCO7190*, and *NovQ*) and *S. flavescens* genes (*N8DT* and *G6DT*) were used for the targeted production of prenylated polyphenols. We modified the subcellular localization of prenyltransferases to express them in the cytosol, plastids, and mitochondria for soluble-type prenyltransferases from Streptomyces (NphB, SCO7190, and NovQ). A total of 624 transgenic *L. japonicus* were generated and analyzed for the production of prenylated polyphenols, and the effect of modification of the subcellular compartmentation of prenyltransferases on the production of prenylated polyphenols was evaluated.

Leaves of transgenic plants were extracted with methanol for chemical analysis using liquid chromatography/mass spectrometry (LC/MS). Unfortunately, none of the transgenic lines accumulated a detectable level of prenylated polyphenol in the leaves. We then supplemented naringenin (100 μM) or genistein (100 μM) to transgenic leaves and incubated for 24 hours before extraction. 7-*O*-geranylgenistein was detected in transformants with plastid-localized NphB, but not detected in transformants with cytosol-localized or mitochondria-localized NphB. Both 6-dimethylallylnaringenin and 6-dimethlallylgenistein were detected in plastid-localized SCO7190 transformants; however, these products were not detected in transformants with cytosol-localized and mitochondria-localized SCO7190. Following incubation with 100 μM naringenin and genistein, N8DT transformants produced 8-dimethlallylnaringenin, the direct enzyme reaction product, and G6DT transformants produced 6-dimethylallylgenistein. The overexpression of prenyltransferases in plants yielded only low levels of prenylated polyphenols even after supplementation of the substrate. For *in vivo* prenylation, plastids are the most suitable subcellular compartment for prenyltransferases, both for soluble and membrane bound types. At the same time the problems to be solved are also pointed out, e.g. higher supply of both substrates (i.e. DMAPP and polyphenols). One new strategy will be plastid transformation for the higher production of prenylated polyphenols.

Acknowledgements

We thank Dr. Masayoshi Kawaguchi of the National Institute for Basic Biology for valuable advice on the transformation of *L. japonicus*. We thank Dr. Toshio Aoki of Nihon University, Dr. Hirobumi Yamamoto of Toyo University, Dr. Satoshi Mishima from API Co. Ltd, and Dr. Tsuyoshi Nakagawa for the gift of A. tumefaciens, dimethylallylated flavonoids, prenylated phenylpropanoids, and pGWB vector, respectively. Seeds of *L. japonicus* were provided by the National BioResource Project.

References

[1] Sugiyama, A., Linley, P.J., Sasaki, K., Kumano, T., Yamamoto, H., Shitan, N., Ohara, K., Takanashi, K., Harada, E., Hasegawa, H., Terakawa, T., Kuzuyama, T., Yazaki, K., "Metabolic engineering for the production of prenylated polyphenols in transgenic legume plants using bacterial and plant prenyltransferases", *Metabolic Engineering*, vol. 13. pp. 629-637, 2011.

RECENT RESEARCH ACTIVITIES

Development of a real-time monitoring system for precipitable water vapor using a dense GNSS receiver network for GNSS/QZSS

(Laboratory of Atmospheric Sensing and Diagnosis, RISH, Kyoto University)

Kazutoshi Sato, Eugenio Realini, Masanori Oigawa, Yuya Iwaki, and Toshitaka Tsuda

Because of global warming, the frequency and intensity of extreme weather events are projected to increase, leading to serious hydrological hazards such as landslides, unexpected increases in river level. Torrential rains in urban areas, resulting from the sudden development of a strong thunderstorm associated with sudden heavy rainfall, are becoming a serious problem. The horizontal scale of local heavy rainfall is as small as a few kilometers; it is difficult to predict such rainfall from the current numerical weather forecasts. Weather radar can detect a cloud only after the event becomes evident. An observation system to monitor the behavior of water vapor before the formation of clouds is, hence, necessary.

A Global Navigation Satellite System (GNSS), represented by a GPS, is now widely used for the precise determination of coordinates. The ultimate error in satellite positioning arises from the propagation delay of the GNSS radio signal within the atmosphere. The delay can, however, be related to the accumulated water vapor along the signal path, which can be mapped in the vertical direction to estimate the precipitable water vapor (PWV). This is the basic concept of GPS meteorology.

In a conventional GPS meteorological method, all available GPS satellites above an elevation angle of 5–10° are used to estimate PWV; therefore, the horizontal resolution of GPS-PWV is as wide as about 20 km. We here propose to use GNSS satellites at high elevation angle only, thus improving the horizontal resolution of the PWV estimates considerably. In particular, we will employ the Quasi-Zenith Satellite System (QZSS), which was launched in September 2010 by JAXA. One of the QZSS satellites is positioned over Japan continuously for about 8 hours daily, and hence, it is suitable for monitoring PWV with a better horizontal resolution than in conventional methods.

We have installed a dense GNSS receiver network (10–15 GNSS/QZSS receivers) with a horizontal spacing of 1–2 km around the Uji campus of Kyoto University. Comparison tests between GPS-derived PWV, radiometer PWV, and radiosonde PWV were carried out during July and August 2011. Within the range of 1–4 mm, the GPS-PWV PWV agrees with the PWV derived from radiosondes and the radiometer. We will employ this system to study extreme weather events in the tropical regions in future.

Acknowledgements

This research is supported by the Coordination Funds for Promoting Space Utilization of the Ministry of Education, Culture, Science and Technology (MEXT).

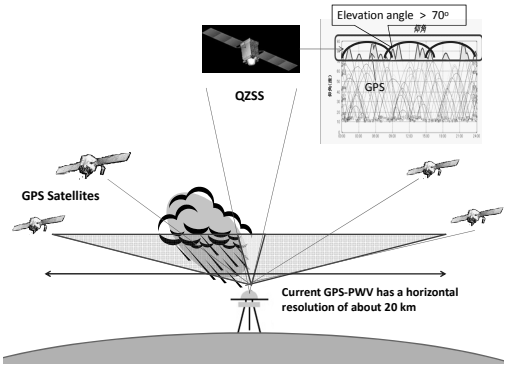

Figure 1. A horizontal water vapor monitoring system employing a GPS and the QZSS.

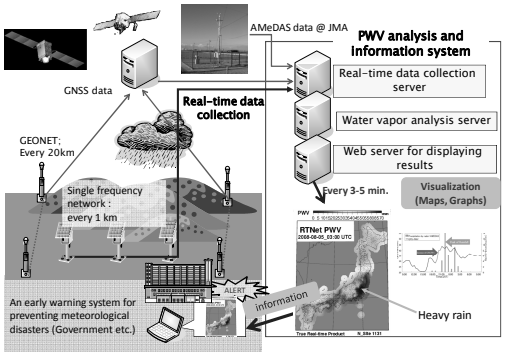

Figure 2. A schematic of a GNSS-based weather forecast early warning system

RECENT RESEARCH ACTIVITIES

Dry Deposition and Oligomerization of Gaseous Isoprene on Atmospheric Water's Surfaces

(Laboratory of Atmospheric Environmental Information Analysis, RISH, Kyoto University)

Shinichi Enami

It is estimated that ~0.6 petagrams (10^{15} g) of gaseous isoprene (ISO, 2-methyl 1,3-butadiene) are emitted by the biosphere annually, representing half of volatile organic compound (VOC) emissions. In spite of the magnitude of the number and the anticipated response to global climate change, it is unclear how and how much it is converted to atmospheric aerosols. Current atmospheric chemistry models predict that ISO emissions atop forest canopies would deplete the oxidizing capacity of the overhead atmosphere, at variance with field observations. Here we address this key issue in novel laboratory experiments where we apply electrospray mass spectrometry [1-3] to detect online the products of the reactive uptake of gaseous ISO on the surface of water jets. We found that ISO is already protonated to $ISOH^+$ and undergoes cationic oligomerization to $(ISO)_2H^+$ and $(ISO)_3H^+$ on the surface of pH < 4 water jets. We estimate uptake coefficients, $\gamma_{ISO} = (0.5 – 2.0) \times 10^{-6}$ on pH = 3 water, which translate into the significant reuptake of leaf-level ISO emissions in typical (surface-to-volume ~5 m^{-1}) forests during realistic (a few minutes) in-canopy residence times (Fig. 1). Our findings also account for the rapid decay of ISO in forests after sunset and help bring the global budget of VOC closer to balance [4].

References

[1] Enami, S., *et al.*, "Acidity enhances the formation of a persistent ozonide at aqueous ascorbate/ozone gas interfaces" *Proc. Natl. Acad. Sci. U.S.A., 105*, 7365-7369, **2008**.

[2] Enami, S., *et al.*, "Proton availability at the air/water interface" *J. Phys. Chem. Lett., 1*, 1599-1604, **2010**.

[3] Enami, S., *et al.*, "Hofmeister effects in micromolar electrolyte solutions" *J. Chem. Phys., 136,* 154707 (5 pages), **2012**.

[4] Enami, S., *et al.*, "Protonation and oligomerization of isoprene on weakly acidic water – Implications for atmospheric chemistry" *J. Phys. Chem. A*, *116*, 6027-6032, **2012**.

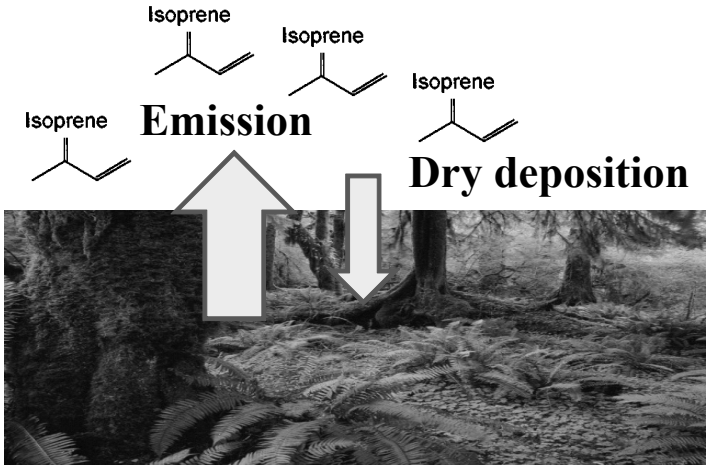

Figure 1. Schematic diagram of the emission and dry deposition of isoprene in the biosphere.

RECENT RESEARCH ACTIVITIES

Development of 1.3-GHz range imaging wind profiler radar

(Laboratory of Radar Atmospheric Science, RISH, Kyoto University)

Masayuki K. Yamamoto, Toshiyuki Fujita, Noor Hafizah Binti Abdul Aziz,
Hiroyuki Hashiguchi, and Mamoru Yamamoto

Radar wind profiler (WPR) is a useful means to measure altitude profiles of vertical and horizontal wind velocities in the clear air. Because WPR receives echoes from Bragg-scale refractive index perturbations caused by turbulence, WPR is able to be used for measuring atmospheric turbulence. However, vertical resolution of WPR (typically 100 m or more) is not sufficient for measuring atmospheric turbulence quantitatively. Range imaging (RIM), which is useful for resolving fine-scale structure of atmospheric turbulence such as Kelvin-Helmholtz billows, has developed recently. RIM improves range resolution down to several ten meters by using frequency diversity and adaptive signal processing. At Shigaraki MU Observatory Japan, we are developing a 1.3-GHz range imaging WPR (RIM-WPR) in order to realize turbulence measurement in the lower troposphere. Antenna, transmitter, and receiver of the existing WPR (named as LQ7) are used for RIM-WPR. To transmit multiple frequencies, five local oscillators (1357.0-1358.0 MHz with 250 kHz intervals) are installed. Further, for collecting received time series every transmitted frequency, we newly developed a radar software receiver using Universal Software Radio Peripheral 2 (USRP2). In addition to the functions necessary for performing the multi-frequency data collection, the new radar software receiver is able to execute oversampling with a maximum sampling rate of 10 MHz. Combining RIM and oversampling provides a sufficient capability to detect small-scale turbulence with a scale 100 m or less.

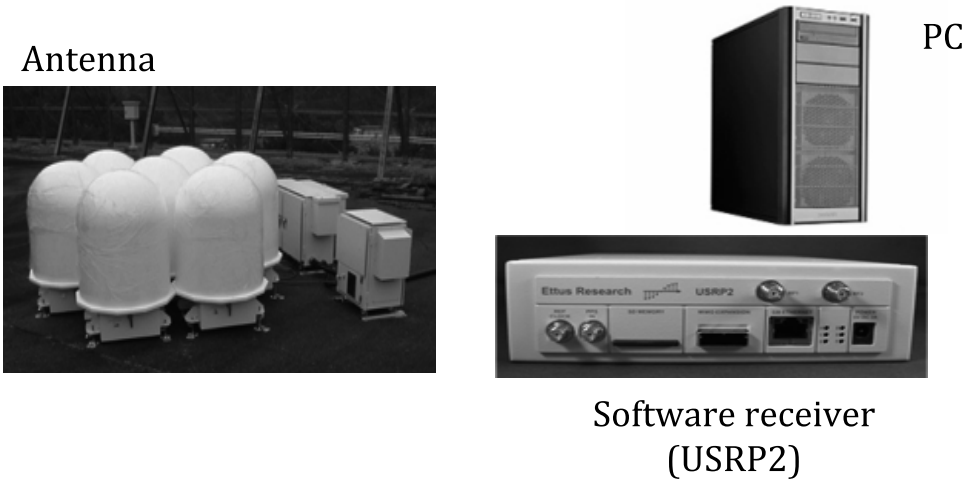

Figure 1. Components of the 1.3-GHz range imaging wind profiler radar.

Acknowledgements

This research was supported by Adaptable and Seamless Technology Transfer Program through Target-Driven R&D (A-STEP) Exploratory Research (Research No. AS232Z00186A).

RECENT RESEARCH ACTIVITIES

Cellulose nanofiber-based hydrogels with high mechanical strength

(Laboratory of Active Bio-based Materials, RISH, Kyoto University)

Kentaro Abe and Hiroyuki Yano

Cellulose nanofibers, which can be isolated from any plant sources by mechanical and/or chemical fibrillation processes, have great potential for reinforcing polymer matrices because of excellent mechanical properties, low weight, large specific surface areas and high aspect ratios. Furthermore, the crystalline nanofibers behave in water like dissolved polymers and homogeneously disperse in water without aggregation and sedimentation although cellulose is insoluble in water.

By taking advantage of the unique nature of the nanofiber suspension, we recently found the easy preparation of hydrogels from cellulose nanofibers through alkaline treatment [1, 2]. Unlike traditional polymer hydrogels, the nanofiber hydrogels could be prepared without dissolving in specific solvents and consisted of a highly porous and crystalline nanonetwork capable of having two different kinds of crystal form of cellulose I and II in response to the increasing concentration of alkaline solutions.

The two types of hydrogels with different crystal forms (cellulose I and II) exhibited high Young's modulus and high tensile strength because of the crystalline network in the gels (Figs. 1 and 2). The nanofiber hydrogel with a cellulose II crystal structure had a continuous network formed by the interdigitation of the neighboring cellulose nanofibers and showed higher tensile properties than the hydrogel with a cellulose I crystal structure. Although recently there have been a few other reports on the preparation of stiff hydrogels from cellulose nanofibers, the gel formation by the interdigitated nanofibers is a unique and interesting finding in this study.

Hydrogen bonds or chemical linkages between cellulose nanofibers are probably not powerful enough to support a high tensile force acting on cellulose nanofibers; however the rigid interdigitated linkage can support the high tensile property inherent in cellulose nanofibers. Paradoxically, the high mechanical properties of the nanofiber hydrogel with a cellulose II crystal structure provides supportive evidence for the interdigitation between cellulose microfibrils with opposite polarities.

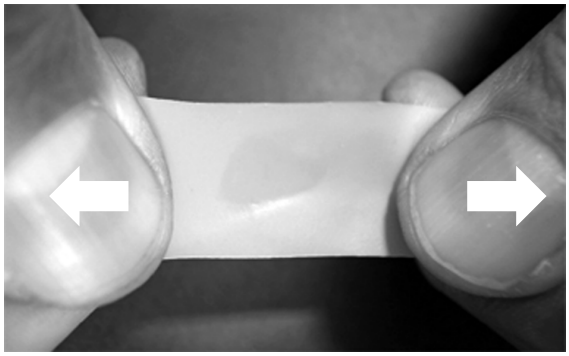

Figure 1. Appearance of the nanofiber hydrogels prepared in 15 wt% NaOH

Cellulose nanofibers are quite strong under tensile stress but rather weak when subjected to compression or bending, resulting in low compressive properties of the hydrogels prepared from cellulose nanofibers. The double-network method, which is a combination of the cellulose nanofiber gels with natural polymers and polysaccharides, is practical and useful for improving poor mechanical properties such as compressive modulus and strength.

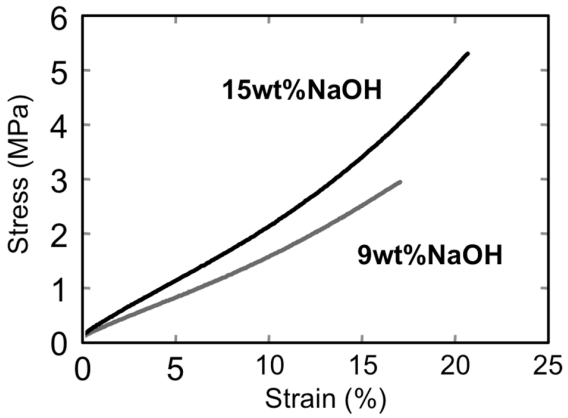

Figure 2. Tensile stress–strain curves of the nanofiber hydrogels prepared in 9 and 15 wt% NaOH.

References

[1] Abe, K., Yano, H. "Formation of hydrogels from cellulose nanofibers" *Carbohydrate Polymers* **85**, 733–737, 2011

[2] Abe, K., Yano, H. "Cellulose nanofiber-based hydrogels with high mechanical strength" *Cellulose*, DOI 10.1007/s10570-012-9784-3, 2012.

RECENT RESEARCH ACTIVITIES

Evaluation of the VOC of Sugi (*Cyptomeria japonica*) wood on psychophysiological responses

(Laboratory of Sustainable Materials, RISH, Kyoto University)

Eri Matsubara, Kenji Umemura, Shuichi Kawai

The volatile organic compounds (VOC) of wood are mainly sesquiterpenes and have strong physiological activities partly. The previous studies have reported that the VOC of several wood materials have the various effects on human body. In this study, we are trying to evaluate the VOC of sugi (*Cyptomeria japonica*) wood on psychophysiological responses. The purpose of our study is to make comfortable living spaces by wood and to increase utility value of wood.

Analysis of VOC in room with Sugi wood

To establish the analysis method of VOC emitted from Sugi wood in a living space, the experimental room of galvanized steel (inside dimension: W1560 × D1840 × H1975 mm) was used. The Sugi wood from Oguni (Kumamoto, Japan) was used as an experimental material. The material was dried at 45 °C and processed to vertical grained timbers (W105 × D12 × L1950 mm). Then, slitting processing was performed as shown in Fig. 1. The ceiling and walls of an experimental room was covered by the slitted sugi timbers. The VOC in this room were collected with a carbon tube (ORBO91T, Supelco, Bellefonte, PA) maintained at 25.8 ± 0.2 °C by applying a flow rate of 0.1 L min^{-1} for 3 h. The VOC were eluted by acetone and analyzed by a GC-MS system (GCMS-QP2010; Shimadzu Co., Ltd., Kyoto, Japan). The machine was equipped with an Ultra ALLOY-5 capillary column (30 m × 0.25 mm i.d., 0.25 μm film thickness; Frontier Laboratories Ltd., Fukushima, Japan). The temperature program was as follows: 50°C for 3 min, followed by increases of 10 °C/min^{-1} to 250 °C, and holding for 5 min. The other parameters were as follows: injection temperature, 250 °C; ion source temperature, 250 °C; carrier inlet pressure at 100 kPa; He at 1.69 mL min^{-1}; injection volume, 1 μL. The GC-MS chromatogram of VOC emitted from Sugi wood were shown in Fig. 2. We compared the GC-MS data with mass spectral database library (NIST08) and previous study [1] for substance estimation. As a result, the VOC were mainly composed of α-cubebene, β-cubebene, α-muurolene, δ-cadinene and other several sesquiterpenes. We are just preparing to identify the compounds by retention index with *n*-alkanes and commercially available reagents. And then, we calculate the concentrations of the target compounds in the sample using the calibration standard line of these reagents.

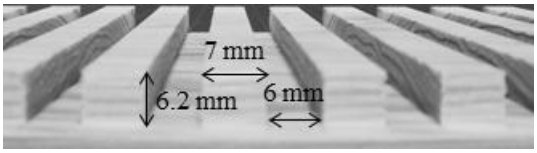

Fig. 1 Sugi wood materials with slitting

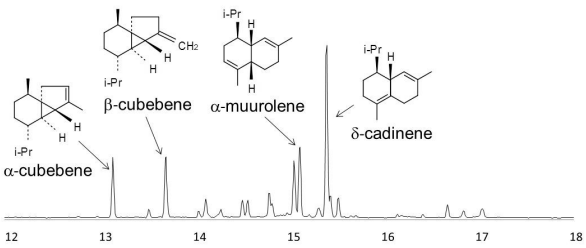

Fig. 2 GC-MS Chromatogram of VOC emitted from Sugi wood

Evaluation of VOC emitted from Sugi wood on psychophysiological responses

We are preparing to evaluate the influences on human body by breathing the VOC in the room with Sugi wood. The evaluation indices of human body are temporal changes of heart rate intervals and autonomic nerve activity as measured by electrocardiography, and subjective assessment for VOC, work performance with arithmetic work, salivary hormones.

References

[1] Ohira T etc "Evaluation of dried-wood odors: comparison between analytical and sensory data on odors from dried sugi (*Cyptomeria japonica*) wood", *J Wood Sci*, vol. 55, pp. 144-148, 2009.

RECENT RESEARCH ACTIVITIES

New Proposal for Enhancing Seismic Performance of Traditional Wooden House by Using Sheathed Wooden Lattice Walls or/and Built-Up Box-Beams

(Laboratory of Structural Function, RISH, Kyoto University)

Kohei Komatsu, Takuro Mori and Akihisa Kitamori

Even now in japan, a lot of wooden dwelling houses are not enough in their seismic performances for servings from devastating earthquake attacks; especially many of traditional wooden houses may have this tendency. It is, however, not always better to let their seismic performance enhanced by subjected to modern reinforcement method rigorously so as to meet with current requirement in Building Bylaw, because modern reinforcement method tends to destroy better features of traditional building style. In order to enhance seismic performance of traditional wooden house with keeping its better features, we proposed a new construction method as shown in Fig.1 by adding not only ①aesthetic sheathed wooden lattice shear wall but also ②built-up beam in upper space or/and ③under floors, just putting portal frame on the base stones without connecting tightly to reinforced concrete base using anchor bolts. In this construction method, lateral resistance of all structural elements were assumed to be ensured by the friction resistance force which was brought by vertical dead load from such upper layer as heavy roof tiles with mud.

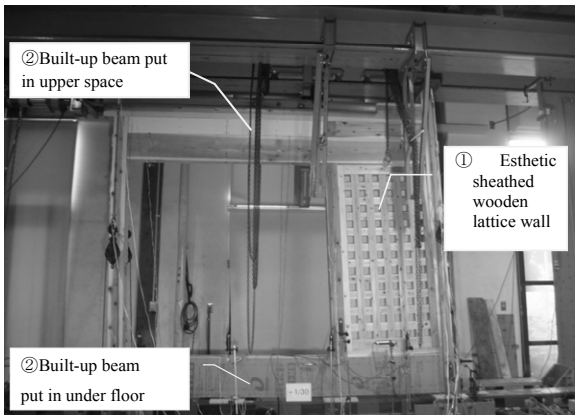

Fig.1 Concept of new seismic reinforcement method

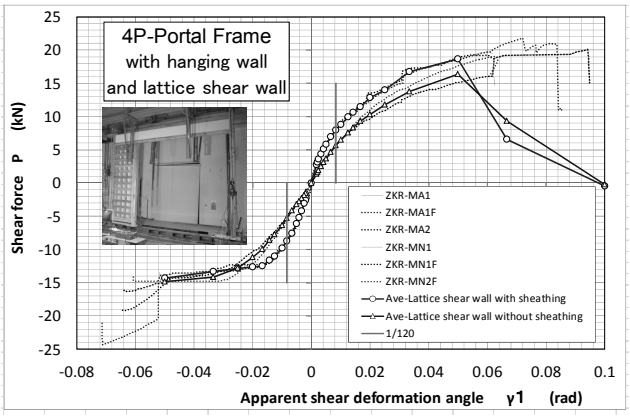

Fig.2 Load-deformation curves

Figure 2 shows typical examples of load-shear deformation angle relationship (envelope curves) of seismic resisting portal frames with hanging wall and wooden lattice shear wall, just putting on the stone base subjected to vertical loads for simulating roof load. By taking these research results into structural design procedure, a traditional wooden house was rebuilt as shown in Figs.3 and 4 in a portion of "Preservation Districts for Groups of Traditional Buildings" of Tondabayshi-City, Osaka prefecture on March in 2012. Our research result could be fruited successfully in an actual wooden house renovation.

Fig.3 Inside view of the house under construction.

Fig.4 Outside view before renovation

RECENT RESEARCH ACTIVITIES

Comparison of behavioral changes in the termite, *Coptotermes formosanus* (Isoptera), inoculated with six fungal isolates

(Laboratory of Innovative Humano-Habitability, RISH, Kyoto University)

Aya Yanagawa

Hygiene behaviors in termites play an important role to protect the insect from pathogenic infection. To clarify the termite behavioral responses after their contact with pathogens, we compared behavioral changes in the subterranean termite *Coptotermes formosanus* caused by contact with entomopathogenic fungi with different levels of virulence.

When untreated termites were allowed to contact their fungus-inoculated nestmates, mutual grooming was frequent during 30 min after inoculation. Since the inoculated termite were often attacked and eaten by their uninoculated nestmates, and then buried after death, these behaviors were also examined. Although no influence of fungal virulence were observed in these behaviors, the fungal isolates and genera affected not only the frequency of the mutual grooming behavior but also the horizontal transmission pattern, the number of dead individuals and the survival period before the first death following infection. The results indicated that the pathogen-resistance behaviors of termites are affected by features associated with genera and isolates of fungi, but not by pathogen virulence.

The survey sites and protocols are as follows:

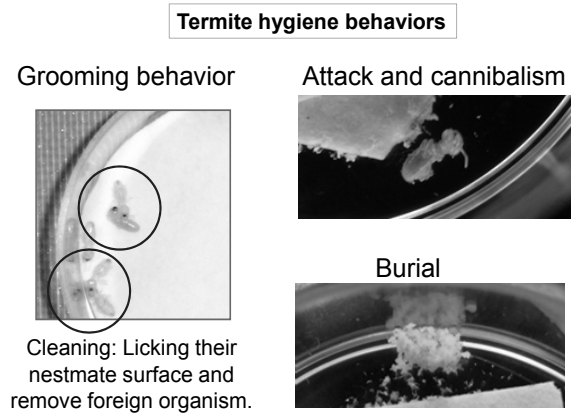

Insects

Matured termites, *C. formosanus*, were obtained from a laboratory colony maintained since 2002 (Okayama, Japan) in the dark at 28 ºC and more than 85% R.H.

Fungi

Three isolates of highly virulent entomopathogenic fungi, *M. anisopliae* 455, *I. fumosorosae* K3 and *B. brongniartii* 782, and three low-virulence isolates, *M. anisopliae* UZ, *I. fumosorosae* 8555 and *B. bassiana* F1214 were selected. Termites show 90–100% mortality on highly virulent fungi and 10-50% mortality on low virulent fungi at 7 days after inoculation, and there are 10- to 100-fold difference in LD_{50} between lower- and higher- virulence fungi when 5 termites are kept in a dish.

Bioassay

Termite behaviors were observed daily under the microscope and compared between fungi treated population and non-treated population.

This study provides the first information that termite increased their hygiene behaviors to resist against infection of entomopathogenic fungi. Beside the result suggests that the pathogen-resistance behaviors of termites are affected by features associated with genera and isolates of fungi, but not by pathogen virulence.

Acknowledgements

I thank Dr. N. Fujiwara-Tsujii (National Institute of Agrobiological Science, Japan), T. Akino (*Kyoto Institute of Technology, Japan)*, T. Yoshimura (Kyoto University, Japan), T. Yanagawa (Kurume University, Japan), S. Shimizu (Kyushu University, Japan) and the late Dr. K. Tsunoda (Kyoto University, Japan) for his helpful supports and collaborations on this study.

The work was published in Journal of Invertebrate Pathology (2011) 107: 100-106.

RECENT RESEARCH ACTIVITIES

Simulations and Modeling of Geospace Environment

(Laboratory of Computer Space Science, RISH, Kyoto University)

Yoshiharu Omura and Yusuke Ebihara

We study space environment surrounding the Earth (geospace) using a large scale computer simulations. Based on the simulation results obtained from the supercomputing on the KDK system, we have developed the nonlinear wave growth theory of whistler-mode chorus waves [1,2] and electromagnetic ion cyclotron waves [3] observed in the inner magnetosphere including the radiation belts. The methods of the simulations are electromagnetic-full particle codes, hybrid code, Vlasov hybrid code, and test particle simulations. While the electromagnetic particle codes have successfully reproduced chorus emissions [4, 5] with reduced space and time models, the hybrid code simulation has reproduced the EMIC triggered emissions with real parameters [6]. The Vlasov hybrid code has also reproduced chorus emissions with both rising-tone and falling-tone emissions. Based on an analysis with the Vlasov hybrid code, we developed a theory of triggering the rising-tone emissions [7], as well as falling-tone emissions. [8]. Chorus emissions can accelerate electrons to relativistic energy (MeV). The relativistic electrons are scattered into the auroral atmosphere by EMIC rising-tone emissions very effectively [9].

By using particle data acquired by the Polar satellite, we found that the number of the ions constituting the ring current is increased, decreased, or unchanged, depending on kinetic energy and magnetic local times during the magnetic storms [10]. An interesting feature is that high energy ions with energy greater than 125 keV are increased during the storm recovery phase. This is opposite to the low energy ions. Our study suggests that energetic ions may have a point in common with high energy electrons. By performing a computer simulation, we found that a rapid decay of the ring current can be reasonably explained by pitch angle scattering of energetic ions in the stretched magnetic field [11]. Recently, we have also developed the drift kinetic simulation that solves transport of relativistic electrons in the inner magnetosphere. By incorporating with the large-scale electric and magnetic fields provided by a global magnetohydrodynamics (MHD) simulation, we found that the relativistic electrons are redistributed by two types of electric fields that are self-consistently induced in the inner magnetosphere in the course of substorms. Our simulations suggest that the force-induced processes, which are self-consistently coupled to the electromagnetic processes, play an essential role in the substorm-associated redistribution of particles in the radiation belt.

References

[1] Omura, Y.,Y. Katoh, and D. Summers, Theory and simulation of the generation of whistler-mode chorus, J. Geophys. Res., 113, A04223, 2008.; [2] Omura, Y., M. Hikishima, Y. Katoh, D. Summers, and S. Yagitani, Nonlinear mechanisms of lower band and upper band VLF chorus emissions in the magnetosphere, J. Geophys. Res., 114, A07217, 2009. ; [3] Omura, Y., J. S. Pickett, et al., Theory and observation of electromagnetic ion cyclotron triggered emissions in the magnetosphere, J. Geophys. Res., 115, A07234, 2010. ;[4] Katoh, Y., and Y. Omura , Amplitude dependence of frequency sweep rates of whistler mode chorus emissions, J. Geophys. Res.,116, A07201, 2011.; [5] Hikishima, M., and Y. Omura, Particle simulations of whistler-mode rising-tone emissions triggered by waves with different amplitudes, J. Geophys. Res., 117, A04226, 2012.; [6] Shoji, M., and Y. Omura, Simulation of electromagnetic ion cyclotron triggered emissions in the Earth's inner magnetosphere, J. Geophys. Res., 116, A05212, 2011.; [7] Omura, Y., and D. Nunn, Triggering process of whistler mode chorus emissions in the magnetosphere, J. Geophys. Res., 116, A05205, 2011.; [8] Nunnn, D., and Y. Omura, A computational and theoretical analysis of falling frequency VLF emissions, J. Geophys. Res., in press.; [9] Omura Y., and Q. Zhao, Nonlinear pitch-angle scattering of relativistic electrons by EMIC waves in the inner magnetosphere, J. Geophys. Res., in press; [10] Temporin, A. and Y. Ebihara, Energy-dependent evolution of ring current protons during magnetic storms, J. Geophys. Res., 116, A10201, doi:10.1029/2011JA016692, 2011. [11] Ebihara, Y., M.-C. Fok, T. J. Immel, and P. C. Brandt, Rapid decay of storm time ring current due to pitch angle scattering in curved field line, J. Geophys. Res., 116, A03218, doi:10.1029/2010JA016000, 2011.

RECENT RESEARCH ACTIVITIES

Microwave Power Transmission to a Sensor Terminal for Wireless Sensor Network

(Laboratory of Applied Radio Engineering for Humanosphere, RISH, Kyoto University)

Tomohiko Mitani and Naoki Shinohara

Wireless sensor network is becoming an attractive application for monitoring systems such as energy conservation systems of buildings and houses, traffic management systems, environment monitoring systems etc. One of the critical issues of the wireless sensor network is the way to supply electric power for sensor terminals. Primary batteris need to be changed soon or later even though power consumption of the sensor terminals is quite small. Natural energy utilization like solar cells with a charging system will drive the sensor terminal permanently; however their installation location and regular operation are limited because the natural energy is quite unstable. We therefore suggest wireless power supply to the sensor terminals by microwave power transmission (MPT), in order to realize a fruitful wireless sensor network.

The objective of the present study is to drive or charge a wireless sensor terminal by MPT. We adopt a ZigBee device as wireless sensor terminal because of its low power consumption. ZigBee is one of the radio communication standards and appropriate for the sensor network for the following reasons: its power consumption is lower than wireless LAN and Bluetooth, its production cost is low, and its network capacity is large. Its low power consumption is beneficial for a MPT system from the viewpoint of electromagnetic compatibility between MPT and ZigBee.

We experimentally investigated electromagnetic compatibility between ZigBee and microwave power transmission, and found that there were some frequencies and power levels of microwave power transmission not to interrupt ZigBee. We also developed a microwave power receiving system which consists of a receiving antenna, a rectification circuit, a dc-dc converter, and a power storage circuit or a secondary battery. Finally we succeeded establishment of ZigBee network while driving a ZigBee device without batteries by microwave power transmission, as shown in Figure 1. Through the experiments, we found out intermittent microwave power transmission was preferable to CW microwave power transmission with respect to electromagnetic compatibility and rf-dc efficiency [1, 2].

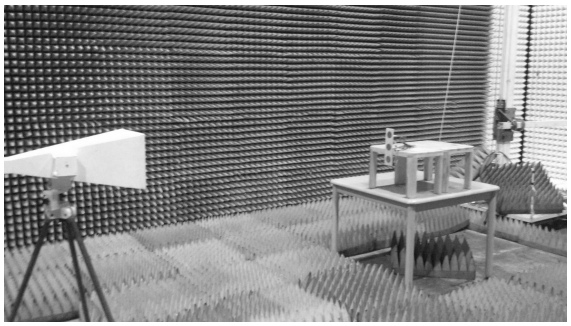

Figure 1. Photograph of intermittent MPT demonstration to a ZigBee terminal.

As future works, we will study on scheduling management between MPT and ZigBee. Although we succeeded intermittent MPT demonstration to a ZigBee device as a feasibility study, scheduling management will be essential for realizing a fruitful wireless sensor network. Also we will have to study how to transmit microwave power to multiple ZigBee devices in a wide area.

References

[1] Suzuki, N., T. Mitani, and N. Shinohara, “Study and Development of a Microwave Power Receiving Circuit for ZigBee Device,” *Proc. of Asia-Pacific Microwave Conference 2010 (APMC 2010)*, pp.45-48, Yokohama, Dec. 2010.

[2] Ichihara, T., T. Mitani, and N. Shinohara, “Study on Intermittent Microwave Power Transmission to a ZigBee Device,” *Proc. of 2012 IEEE MTT-S International Workshop Series on Innovative Wireless Power Transmission: Technologies, Systems, and Applications (IMWS-IWPT 2012)*, pp.209-212, Kyoto, May 2012.

RECENT RESEARCH ACTIVITIES

Wave-Particle Interaction Analyzer onboard ERG satellite

(Laboratory of Space Systems and Astronautics, RISH, Kyoto University)

Hirotsugu Kojima

One of the key targets in the ERG mission is to investigate wave-particle interactions leading to the generation of high energy electrons in the terrestrial radiation belt [1]. The study of wave-particle interactions has been conducted by examining the correlation of wave spectra/waveforms and plasma energy spectra/velocity distributions which are observed by plasma wave receivers and particle detectors, independently. The disadvantage of this method is the difference of the time resolutions of plasma wave data and plasma data. Furthermore, the quantitative data analysis is difficult in this method, because the phase relation between electric field and particle velocity vectors is missing. In order to overcome these disadvantages, we proposed the new method for the direct measurement of wave-particle interactions. It is addressed by Wave-Particle Interaction Analyzer (WPIA) [2]. The WPIA makes use of each pulse which shows the detection of particles in plasma detectors. The WPIA calculates $\boldsymbol{E} \bullet \boldsymbol{V}$ at each timing of particle detection by multiplying instantaneous electric field wave vector (see Figure 1). Since $\boldsymbol{E} \bullet \boldsymbol{V}$ is equivalent to time differential of plasma kinetic energy, the quantitative energy flow among waves and plasmas can be obtained using the WPIA.

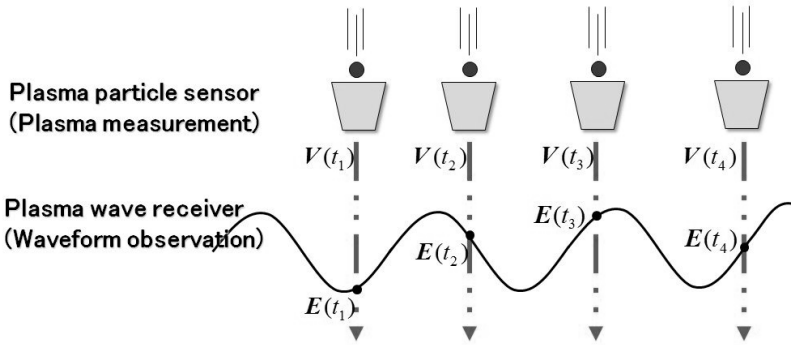

Figure 1. Schematic drawing of the WPIA algorithm.

The WPIA onboard the ERG satellite is realized by the onboard software. The software of the WPIA runs on the digital processing unit addressed MDP (Mission Data Processor). The WPIA needs the information of velocity vectors of sampled particles, instantaneous plasma wave vectors, and the ambient magnetic field vector. These data are stored onto the onboard data recorder through the high speed digital interface called SpaceWire.

The MDP reads out the above data from the data recorder and the WPIA calculates the physical quantity $\boldsymbol{E}_w \bullet \boldsymbol{V}$. The important point in this system is the time accuracy. In order to identify the wave-particle interaction on the chorus emission, we need the time synchronization accuracy is $10\,\mu\mathrm{sec}$ at least. This accuracy will be guaranteed by the synchronization pulse from the system and the high frequency counter installed inside the plasma wave receiver.

The current status of developing the WPIA for the ERG mission is under considering the appropriate algorithm using computer simulations. The computer simulation reproduces the generation process of the chorus emission and the acceleration of electrons by the chorus emission. The algorithm based on the computer simulation will be examined using the breadboard of the MDP designed for the ERG emission.

References

[1] Miyoshi, Y., K. Seki, K. Shiokawa, T. Ono, Y. Kasaba, A. Kumamoto, M. Hirahara, T. Takashima, K. Asamura, A. Matsuoka, T. Nagatsuma, and ERG working group,"Geospace Exploration Mission: ERG project", *Trans. Japan Soc. Aero Space Sci.*, vol.8, ists27, 2010.

[2] Fukuhara, H., H. Kojima, Y. Ueda, Y. Omura, Y. Katoh, and H. Yamakawa, "A new instrument for the study of wave-particle interactions in space: One-chip wave-particle interaction analyzer," *Earth Planets Space*, vol. 61, pp. 756-778, 2009.

ABSTRACTS (PH D THESIS)

Variation of Fiber Properties in Relation to the Distance from Vessels in *Acacia mangium*

(Laboratory of Biomass Morphogenesis and Information, RISH, Kyoto University)

Ridwan Yahya

The *Acacia* plantation in Indonesia requires a tree improvement program to increase the yield of solid wood and its quality to meet market demands. In the plantations operating on Sumatra Island in Indonesia, the plantation program remains primarily in the selection step, and has not yet implemented the breeding step. Another problem of these plantations is that trees are primarily selected based on growth rate and stem form. Hence, the improvement of wood quality to meet end-product requirements is still in progress. For instance, a trial hybrid of *A. mangium* and *A. auriculiformis* are growing. Its stem form and growth rate show that this *Acacia* hybrid is promising, and tends to produce better quality raw material for pulp and papermaking compared to its parents [1]. However, to date, little is known even regarding basic properties, such as density, anatomy, and chemical composition of the hybrid in Indonesia.

The objectives of this study are as follows; (1) evaluating wood properties of the *Acacia* hybrid, in parallel to searching for specific anatomical predictors of pulp yield and paper strength applicable to this species, (2) introducing a facile, quick, and reliable technique to obtain 3D reconstructed data from serial optical micrographs to investigate the above mentioned relationships, and (3) investigating fiber length in tangential direction in relation to the distance of fibers from vessels.

The basic properties of the *Acacia* hybrid were investigated. Compared to both parents, *A. mangium* and *A. auriculiformis*, the *Acacia* hybrid had longer fibers, in addition to a higher slenderness ratio, fiber proportion, and holocellulose content, but smaller proportions of vessels, parenchyma cells, and extractives. In addition, the hybrid tended to have a thinner cell wall, and a lower proportion of ray cells, rigidity, and lignin content, but a higher flexibility coefficient and wood density compared to *A. mangium* (Tables 1,2). Fiber length was positive & negative correlation with α-cellulose and lignin content, respectively. Holocellulose content was all reliably predicted by fiber length. The slenderness ratio was a better predictor of extractive content than fiber length. Both the fiber length and slenderness ratio were better predictors of chemical composition than wood density. Therefore, fiber length and the slenderness ratio could be used as reliable predictors of pulp yield and paper strength for acacias.

Table 1. Fiber dimension and derived values of *Acacia* hybrid and its parents

Species	FL (μm)	FD (μm)	FLD (μm)	FWT (μm)	RR	MR	SR	CR	FC	PF (%)	PR (%)	PP (%)	PV (%)
Acacia hybrid	1068	18.76	13.74	2.51	0.37	46.17	57.4	0.13	0.73	72.65	8.51	9.39	9.45
A. mangium	982**	19.39	14.29	2.55	0.37	45.85	51.29*	0.13	0.73	62.46**	9.77	15.66*	12.11**
A. auriculiformis	879**	16.74*	11.13*	2.81	0.55	55.00	52.65*	0.17	0.67	68.18*	9.07	11.23	11.55**

FL = fiber length, FD = fiber diameter, FLD = fiber lumen diameter, FWT = fiber wall thickness

RR = Runkel ratio, MR = Muhlsteph's ratio, SR = slenderness ratio, CR = coefficient of rigidity, FC = flexibility coefficient

PF, PR, PP, PV = Proportions of fiber, ray cells, parenchyma cells and vessels respectively

** Significantly different at the 0.01 level, * = at 0.05 level

Next, I focused on a more detailed search of the anatomical factors, with special reference to fiber length by exploring *A. mangium*. A newly developed 3D microscopy technique was introduced to create aligned serial images from the cross sectional micrographs. Reconstruction of 200 serial images took just 1 day, and all digital information was compiled in a personal computer. This dataset allowed us to quickly and easily estimate wood fiber length using a public-domain software. It took no more than 2 min to locate the 2 tips of a fiber, by scrolling images on the computer, which contrasts against previous studies of serial cross sections [2]. Given this technical development, fiber length variation in relation to the distance from

vessels was measured in detail. Fibers that were more distant from vessels were found significantly longer, not only in the radial direction, but also in the tangential direction (Figure 1).

Table 2. Chemical compositions and wood density of Acacia hybrid and its parents

Species	Alcohol–benzene extractives (%)	Holocellulose (%)	α-Cellulose (%)	Lignin (%)	Density (g cm-3)
Acacia hybrid	2.9	82.88	45.45	30.91	0.49
A. mangium	5.38**	80.43**	45.71	31.30	0.46
A. auriculiformis	5.96**	71.33**	40.57*	34.10	0.52

** Significantly different from Acacia hybrid at the 0.01 level, * = at the 0.05 level

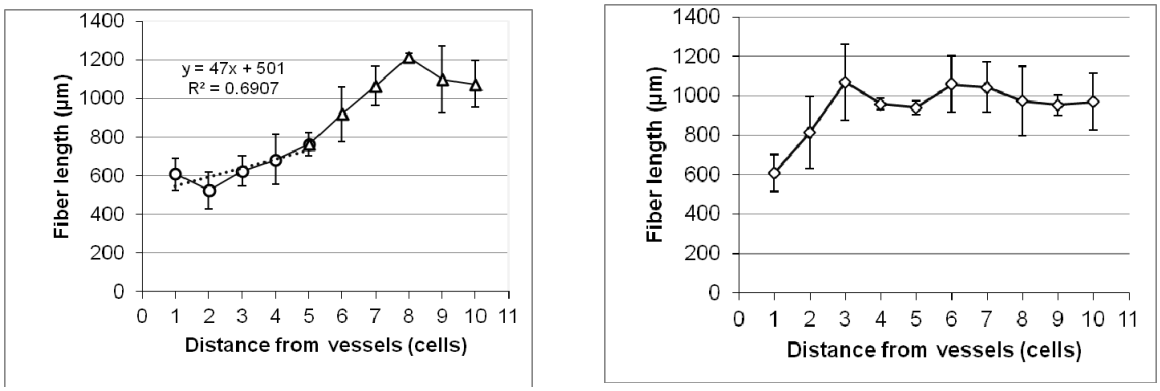

a **b**

Fig. 1. Fiber length variation in (a) radial and (b) tangential directions.

In search of the superiority of *Acacia* hybrid than its parents as a resource for pulp and papermaking, the microstrucre of *A. mangium* were thouroughly investigated, vessels influence the anatomical features such as length in both the radial and tangential direction, although these influences were more tailed in the radial direction. Therefore, to produce high quality pulp and paper, I suggest that the quantity of vessels in the *A. mangium* tree should be reduced through tree improvement breeding programs.

REFERENCES

[1] Yahya, R., J. Sugiyama., D. Silsia & J. Gril. 2010. J. Trop. For. Sci. 22: 343--351.
[2] Yahya, R., K. Koze & J. Sugiyama. 2011. IAWA J. 32: 341--350

ABSTRACTS (PH D THESIS)

Aromatic prenylation in the biosynthesis of bitter acids of hop (*Humulus lupulus* L.).

(Graduate School of Agriculture, Laboratory of Plant Gene Expression, RISH, Kyoto University)

Yusuke TSURUMARU

Hop (*Humulus lupulus* L., Cannabinaceae) is a perennial and dioecious climbing plant and female plants of the species are cultivated world-wide for use as an essential ingredient of beer. Female flowers, also called hop cones, give the characteristic flavor and bitter taste to beer due to a variety of essential oils and aromatic compounds, which are biosynthesized and accumulated exclusively in yellow glandular trichomes, also designated lupulins, which develop at the basal part of hop cone bracts. Among the secondary metabolites produced by the hop plant, prenylated acylphloroglucinols, conventionally called 'bitter acids', have received a large amount of attention because their characteristic bitter property is important for beer taste; moreover, their divergent biological activities, including radical scavenging activity, angiogenesis inhibition, and inducing effect for P450 enzyme, are beneficial for human health. Hop cones also contain prenylated flavonoids, among which the major one is xanthohumol, a prenylated chalcone derivative, which has potential applications as a cancer chemopreventive agent. The proposed biosynthetic pathway of bitter acids in hops, also called α- and β-acid (humulone and lupulone, respectively), are shown in Fig. 1, with the biosynthesis of xanthohumol illustrated in parallel. In the biosynthesis of these secondary metabolites in hops, aromatic prenyltransferases play a crucial role for both phloroglucinol and flavonoid derivatives. The plant prenyltransferases that recognize aromatic secondary metabolites are a new topic of research in plant molecular biology; the first flavonoid-specific prenyltransferase, naringenin 8-dimethyallyltransferase (SfN8DT), was identified in 2008, and thereafter a pterocarpan and isoflavonone-specific prenyltransferases, glycinol 4-dimethylallyltransferase (G4DT) and genistein 6-dimethylallyltransferase (SfG6DT), respectively, have been reported. These enzymes are all divalent cation-requiring membrane-bound proteins, and those characterized to date have been localized in plastids.

In this study, we constructed a cDNA library from the lupulin gland-rich portion of female flower bracts, and randomly sequenced 11,233 EST clones, obtaining sequence information for 6613 non-redundant ESTs. Among them, a cDNA designated Humulus lupulus prenyltransferase-1 (HlPT-1) was a candidate for the gene coding for prenylation enzyme as it possessed three features of the plant aromatic prenyltransferase family, namely, a D-rich motif, multiple membrane-spanning domains, and a putative transit peptide sequence at the N-terminus. Indeed, HlPT-1 was highly expressed in hop cones, especially in the lupulin glands. Moreover, a GFP fusion experiment showed that the transit peptide of HlPT-1 actually localized the GFP fusion protein to plastids in a manner similar to other flavonoid prenyltransferases in the legume plants. Subsequently, we heterologously expressed HlPT-1 protein in insect cells and demonstrated its enzymatic function in vitro assays using phloroglucinol derivatives and various flavonoids as prenyl acceptor substrates in the presence of dimethylallyl diphosphate as a prenyl donor.

ABSTRACTS (PH D THESIS)

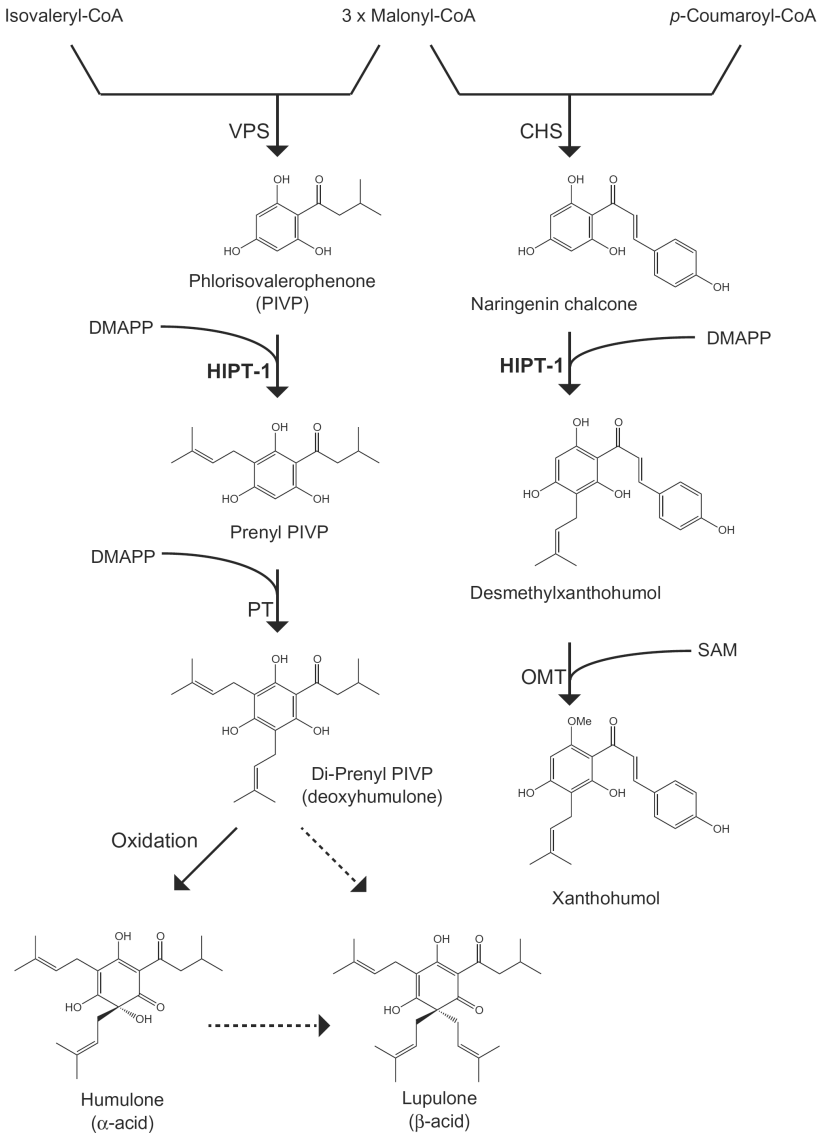

Fig. 1. Biosynthesis of bitter acids (humulone and lupulone) and xanthohumol in lupulin glands of hop.
DMAPP, dimethylallyl diphosphate; VPS, valerophenone synthase; PT, prenyltransferase; CHS, chalcone synthase; OMT, *O*-methyltransferase; SAM, *S*-adenosylmethionine. (modified from Tsurumaru, Y., et al. BBRC, 417, 393-398, 2012)

The HlPT-1 identified in hops catalyzes the first step in prenylation of aromatic substances, adding dimethylallyl moiety to phloroglucinol derivatives and leading to the formation of humulone and lupulone derivatives. HlPT-1 is also responsible for the formation of xanthohumol by transferring prenyl residue to chalcone. Here, we found that HlPT-1 has many characteristic features as an aromatic prenyltransferase that set it apart from other reported members; namely, narrow optimum pH at around neutral pH, sharp preference for Mg^{2+} as a divalent cation, and broad substrate specificity. It is likely that, HlPT-1 recognizes a phloroglucinol portion as the prenyl acceptor, which is a common structure for the A-ring of naringenin chalcone.

ABSTRACTS (PH D THESIS)

Color Change of Lignocellulosic Materials during Natural Aging and Heat Treatment

**(Graduate School of Agriculture,
Laboratory of Sustainable Materials, RISH, Kyoto University)**

Miyuki Matsuo

Introduction

Lignocellulosic materials can be deteriorated by biodegradation, weathering, and natural aging. Their service life, especially of paper and wood, can exceed thousands of years under the proper conditions where biodegradation and weathering are avoided. In such conditions, natural aging becomes a major source of deterioration of the materials. Understanding the mechanism of natural aging is important not only for the purpose of basic research on lignocellulosic materials but also for the preservation and restoration of culturally significant properties made of them.

Natural aging of lignocellulosic materials is considered as ill-defined deterioration which proceeds slowly in the materials under participation of the omnipresent oxygen and water. Some reports have characterized the properties of naturally aged materials in comparison with those of recent materials. However, these reports remain to be the observation of phenomena that occur during natural aging. To understand the mechanism of natural aging within experimentally available time span, heat treatment below thermal decomposition points of the materials has been very useful to accelerate aging.

The objective of this study is to elucidate natural aging of lignocellulosic materials by comparing the property of naturally aged samples with heat-treated samples. Color, which is one of the physical properties that change during natural aging and heat treatment, was elucidated by means of kinetic analysis. Furthermore, as a possible application of heat treatment, heat-treated materials was evaluated as artificially aged materials.

Materials and Methods

The materials used in this study were cellulose filter paper, Chinese Xuan paper, hinoki (*Chamaecyparis obtusa* Endl.) wood, keyaki (*Zelkova serrata* Makino) wood and sugi (*Cryptomeria japonica* D.Don) wood. The specimens were prepared from naturally aged samples stored in the ambient indoor conditions for the aging durations ranged from approx. 35 years (Xuan paper) to approx. 1600 years (hinoki wood). For control and heat-treated samples, specimens prepared from recently manufactured or harvested samples were dried and then heated in an air-circulating oven at 90, 120, 150 and 180°C for the durations of 10 min. (for keyaki and sugi wood at 180°C) to approx. 3 years (for Xuan paper at 90°C). Color was measured by using spectrophotometer and spectroscopic imaging system and expressed in terms of the CIELAB color parameters (L^*, a^*, b^* and ΔE^*_{ab}). Obtained color data were discussed by means of kinetic analysis applying the time-temperature superposition (TTSP) method for accurate analysis. Heat treatment was also applied to make artificially aged Xuan paper which has preferable characteristics for calligraphy. Specimens of Xuan paper were heated in an air-circulating oven at 180°C for the durations ranging from 0.5 hour to 48 hours. A calligrapher subjectively evaluated the quality of heat-treated specimens by brush handwriting. The moisture content and the water

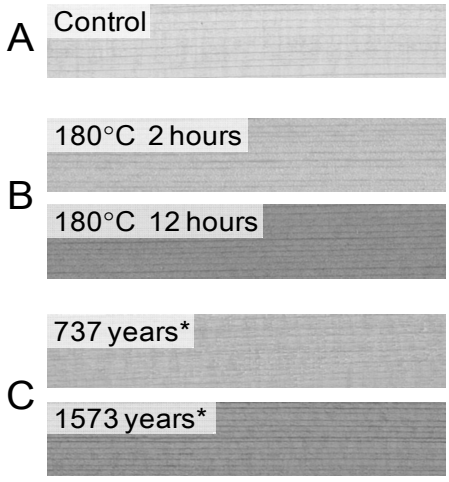

Figure 1. Color changes of hinoki wood during heat treatment and natural aging. A: control (harvested in 1988), B: specimens treated at 180°C for 2 or 12 hours, C: specimens aged in the ambient condition for 737 or 1573 years. *Aging duration was determined by dendrochronology and radio carbon dating.

absorptiveness were also measured as the properties which concern the qualities of paper for calligraphy.

Results and Discussion

As shown in Figure 1 as an example, color changes that occur during natural aging were similar to those during heat treatment for all materials. Color changes were expressed by decreasing L^*, increasing ΔE^*_{ab}, and changes in a^* and b^* characteristic of each material, with increasing treatment duration. Measured color data was successfully analyzed with high accuracy. In the temperature range from 90°C to 180°C, the reaction of color changes followed the Arrhenius equation for all materials, which indicated that color changes in this temperature range can be explained by the apparently same reaction mechanism (Figure 2 (1)) [1]. Comparing color changes measured from naturally aged samples with those at the ambient temperature predicted from kinetic analysis of heat-treated specimens, color changes of hinoki wood during natural aging can be explained mainly as the same reaction as heat treatment, i.e., thermal oxidation (Figure 2 (2)). While, color changes of keyaki wood during natural aging were significantly faster than predicted, suggesting that either thermal oxidation was accelerated or there were other different reactions involved. Color changes and calculated activation energy of cellulose filter paper were similar to those of Xuan paper and wood, indicating that color changes of cellulose significantly contributed to those of Xuan paper and wood [2,3].

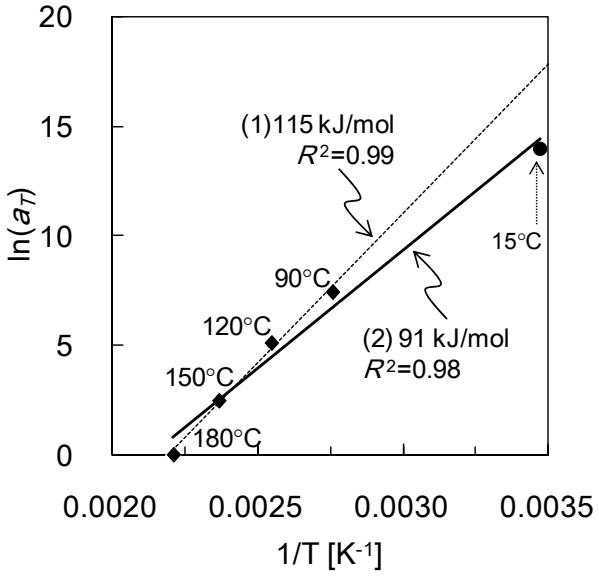

Figure 2. Arrhenius plots of changes in L^* with regression lines, coefficients of determination (R^2) and apparent activation energies calculated from (1) heat-treated hinoki wood and (2) both heat-treated and naturally aged hinoki wood.

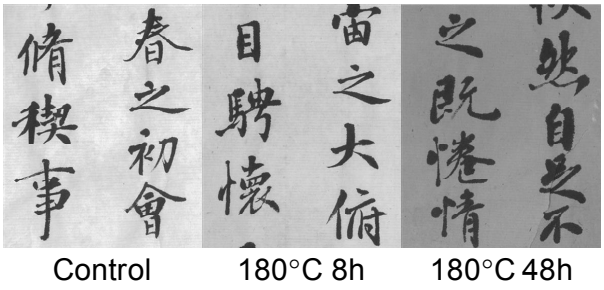

Figure 3. Brush handwriting on heat-treated Xuan paper by a calligrapher (臨書:王羲之「蘭亭序」, Study of a masterpiece: "*Lanting Xu*" by *Wang Xi Zhi*). The numbers below the figure indicate treatment temperature and durations.

Figure 3 shows the heat-treated Xuan paper with brush handwriting by a calligrapher. The calligrapher judged that 3-, 5- and 8-hour-heated specimens had the good quality for calligraphy. Equilibrium moisture contents decreased with the increasing treatment duration. Water absorption of Xuan paper treated for 0.5-8 hours was lower than untreated specimens and then increased with increasing treatment duration. These results indicated that heat treatment with appropriate duration allows to produce Xuan paper which has preferable properties for calligraphy.

References

[1] Matsuo M., Yokoyama M., Umemura K., Gril J., Yano K., and Kawai S., "Color changes in wood during heating: kinetic analysis by applying a time-temperature superposition method", *Appl Phys A*, 99, 1-6, 2010.

[2] Matsuo M., Yokoyama M., Umemura K., Sugiyama J., Kawai S., Gril J., Kubodera S., Mitsutani T., Ozaki H., Sakamoto M., and Imamura M., "Aging of wood: Analysis of color changes during natural aging and heat treatment", *Holzforschung*, 65, 361-368, 2011.

[3] Matsuo M., Umemura K., and Kawai S., "Kinetic analysis of color changes in cellulose during heat treatment", *J Wood Sci*, 58, 113-119, 2012.

ABSTRACTS (PH D THESIS)

Curing and degradation processes of cement-bonded particleboard by supercritical CO_2 treatment

(Graduate School of Agriculture, Laboratory of Sustainable Materials, RISH, Kyoto University)

Rohny Setiawan Maail

Cement-bonded particleboard (CBP) and its application in the building industry have been rapidly accepted in many countries because of its excellent exterior properties. In the development of CBP, many studies have focused on understanding the utilization of carbon dioxide (CO_2) in the manufacturing process [1-6]. This study aimed to evaluate and clarify the curing and degradation processes of CBP under supercritical CO_2 treatment. In order to improve understanding of curing process, the amount of water as a key factor in the production of CBP with CO_2 in the form of supercritical CO_2 was adjusted to determine the optimum condition of moisture content (MC) equaling to certain water-cement (w/c) ratio of boards. Then, CBPs were treated with supercritical CO_2 to provide further evidence and improved understanding of curing and degradation processes.

Considering the properties of CBPs are different when treated by CO_2 in both low and high concentrations compared to the conventional board, the effect of CO_2 at either the gaseous or supercritical phase on the degradation of CBP based on treatment to conventional cured board and estimate long term degradation of these boards affect by gaseous and supercritical CO_2 were also investigated.

Significant correlations were found between the supercritical CO_2 treatment and mechanical properties and dimensional stabilities of CBP during both the curing and degradation processes. Internal bond (IB) strength and modulus of rupture (MOR) values as shown in Figure 1, and modulus of elasticity (MOE) values of CBP achieved their maximums, also thickness swelling (TS) and water absorption (WA) improved significantly by supercritical CO_2 treatment in 30 min. These conditions indicated that supercritical CO_2 treatment accelerates the curing process rapidly and enhances the mechanical properties and dimensional stabilities of CBP.

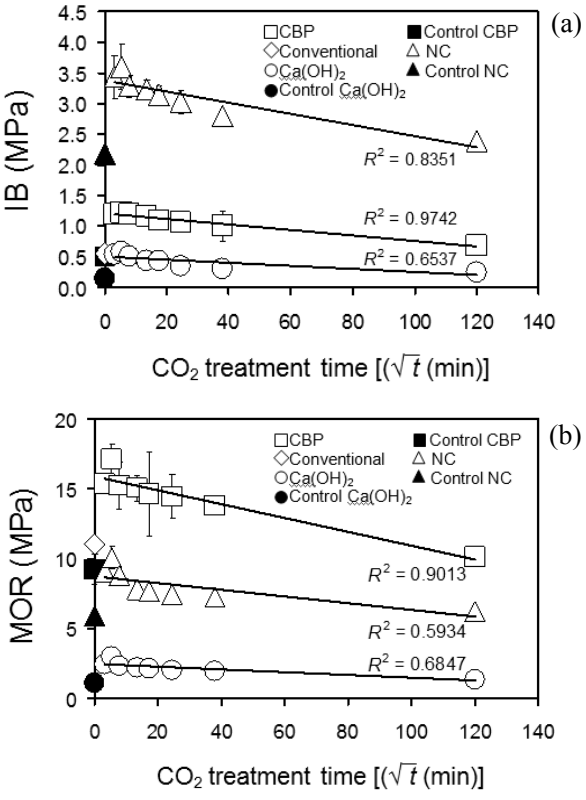

Figure 1. Effect of supercritical CO_2 treatment on the CBP, neat *cement boards (NC) and Ca(OH)$_2$ boards performa*nce at various curing time; **a.** IB, **b**.MOR

During the curing process of manufacturing these boards, a MC of about 30%, which is nearly equal to the water-cement (w/c) ratio of about 0.34, is an ordinary condition of the cement required in curing of CBP, and could promote the reaction of carbon dioxide to form calcium carbonate ($CaCO_3$) which leads to increase in final strength of these boards. However, the mechanical properties and dimensional stabilities of CBP decreased in the treatments from 60 min to 10 days and had a negative effect on the board performance, indicating that supercritical CO_2 treatment over a longer time span leads to the degradation of the CBP. This finding suggests that higher CO_2 consumption, equaling longer treatment time by supercritical CO_2, causes decreased of density,

which suggests the changes of morphological structure of $CaCO_3$ formed in CBP, could account for higher porosity and lead to degradation of CBP (degraded mechanical properties and increased water absorption). Furthermore, X-ray diffractometry (XRD) as shown in Figure 2, also thermal gravimetry (TG-DTG) and scanning electron microscopy (SEM) observation clarified that the mechanisms of the degradation are directly affected by the mineralogical composition of the system, in particular by the calcium carbonate content as caused by carbonation of cement. Moreover, the properties of CBP are improved by CO_2 treatment in both gaseous and supercritical phase even after the conventional curing process. These properties, however, over the longer treatment time degraded in rapid rate against CO_2 treatment in both gaseous and supercritical phase. The times required for degradation of such properties of CBP treated at 10.0 MPa of CO_2 pressure or under supercritical phase was markedly short compared to the times at 1.0 MPa of CO_2 pressure or under gaseous phase. High coefficient determination values between the degradation rates of IB strength, MOR, MOE, TS and WA of CBP, and the treatment time and CO_2 concentration were observed and the simple linear model was found among the properties and affecting factors.

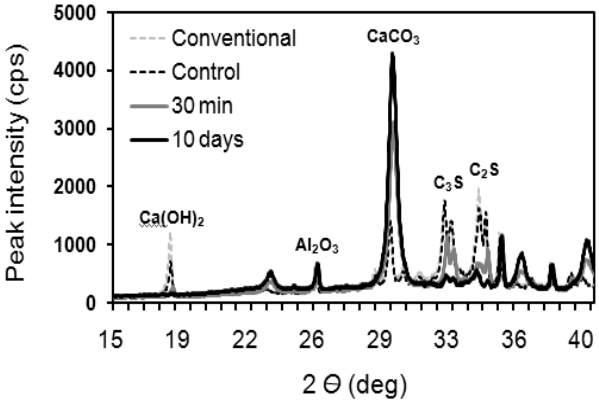

Figure 2. XRD patterns of various curing treatment of CBP

Acknowledgements

This paper is a part of the outcome of the JSPS Global COE Program (E-03) : In Search of Sustainable Humanosphere in Asia and Africa.

References

[1] Simatupang M.H., H. Seddig, C. Habighorst, L. Geimer, "Technologies for rapid production of mineral-bonded wood composite boards," *For Prod J*,2:10-18, 1991.

[2] Geimer L., M.R. Souza, A.A. Moelemi, M.H. Simatupang, "Carbon dioxide application for rapid production of cement particleboard," *For Prod J,* 3:31-41, 1993.

[3] Simatupang M.H., C. Habighorst, "The carbon dioxide process to enhance cement hydration in manufacturing of cement-bonded composites - comparison with common production method," *For Prod J* , 3:114-120, 1993.

[4] Lahtinen P.K., "Experiences with cement-bonded particleboard manufacturing when using a short cycle press line," *For Prod J,* 2:32-34, 1991.

[5] Hermawan D., T. Hata, K. Umemura, S. Kawai, W. Nagadomi, Y. Kuroki, "Rapid production of high-strength cement-bonded particleboard using gaseous or supercritical carbon dioxide," *J Wood Sci* ,47:294-300, 2001.

[6] Qi H., P.A. Cooper, H. Wan, "Effect of carbon dioxide injection on production of wood cement composites from waste medium density fiberboard (MDF)," *Waste Management,* 26:509-515, 2006.

ABSTRACTS (PH D THESIS)

Computer Simulations of Nonlinear Wave Instabilities Driven by Ion Temperature Anisotropy in Space Plasmas

**(Graduate School of Engineering,
Laboratory of Computer Simulation for Humanospheric Sciences,
RISH, Kyoto University)**

Masafumi Shoji

As one of the important phenomena in the space plasmas, instabilities driven by the temperature anisotropy of ions take place. For example, the ions are heated in the perpendicular direction to the ambient magnetic field due to the adiabatic heating in the downstream of the quasi-perpendicular shock. In the inner magnetosphere, there exists the inward transportation of the energetic plasmas due to the magnetic reconnections in the magnetotail. These phenomena form anisotropic velocity distribution functions of the ions in each region. The ion temperature anisotropy in the perpendicular direction drives mirror and electromagnetic ion cyclotron (EMIC) instabilities through the wave particle interactions. The mirror mode structures and the L-mode EMIC waves, which are excited through these instabilities, have large amplitude and scale size and thus they play a significant role for the energy transportations in the different parts of the geospace plasmas. We analyzed the nonlinear evolutions of these waves and interactions with the ions in the Earth's magnetosheath and the inner magnetosphere using the hybrid simulations which treat ions and electrons as particles and fluid, respectively.

The solar winds move through the bowshock, the proton temperature anisotropy causing the mirror and EMIC instabilities arises. Spacecraft observations show that the mirror instability dominates over the L-mode EMIC instability in the magnetosheath, although the theoretical linear EMIC growth rate is higher than that of the mirror mode waves. We performed two- and three-dimensional (2D and 3D) hybrid simulations with the periodic boundary to understand the competing process between the EMIC and mirror instabilities. In the 2D model, the energy of the EMIC waves is higher at the growth phase because of its higher growth rate. In the 3D model, however, the energy of the mirror mode waves is larger than that of the EMIC waves for all times because the wavenumber spectra of mirror mode waves form torus-like structures. As the mirror mode waves relax the temperature anisotropy effectively, the linear growth rates of the EMIC waves become smaller before saturation. The EMIC waves cause heating of protons trapped by the nonlinear potentials due to coexistence of forward and backward propagating waves. They terminate the growth of EMIC waves. Because of the heating, the temperature anisotropy decreases to the threshold of the mirror instability and thus the mirror mode wave saturates. At the nonlinear stage, coalescence of the mirror mode structures takes place in both models. The quick dissipation of the EMIC waves occurs due to the heating by the nonlinear processes. On the other hand, the coalescence is a much slower process than the nonlinear processes of EMIC waves, and thus the mirror mode waves remain.

We also performed 2D and 3D hybrid simulations in open boundary models. In the open systems, because of the propagation of EMIC waves, we obtain the clearer non-propagating mirror mode structures. We analyzed the relation between the mirror instability and the magnetic peaks and dips observed in the magnetosheath. In the 2D model with low beta ($\beta < 1$), we obtain fine structures of the magnetic dips at the nonlinear stage. In the 3D model, on the other hand, the mirror instability makes the magnetic peaks with the same parameters. The parametric analysis indicates that the magnetic peaks also arise in both 2D and 3D high beta cases ($\beta > 1$) as shown by the Cluster observations. In the high beta cases, the high mobility

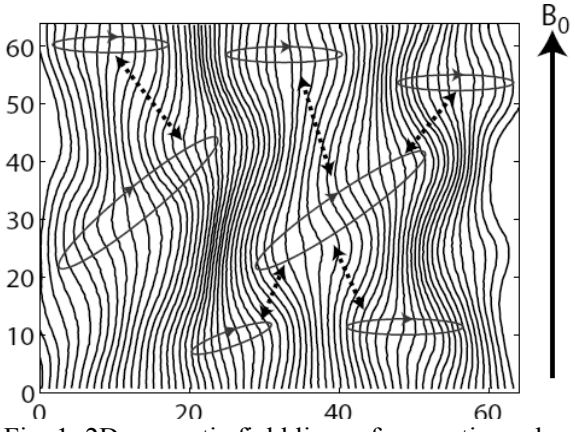

Fig. 1: 2D magnetic field lines of magnetic peak. Red circles show diamagnetic currents.

of the protons helps continuous coalescence of the diamagnetic currents inside the magnetic dips. The coalescence makes the magnetic dips larger and shallower. Between the large and shallow magnetic dips, the magnetic peaks appear in the high beta cases. In the 3D models, because degree of freedom increases in the perpendicular direction, the continuous coalescence can take place even in the low beta cases. Thus, the magnetic peaks appear in the 3D models in both cases.

In the Earth's inner magnetosphere, due to the inward transportation, the EMIC waves are driven. They cause the different nonlinear wave particle interactions because of the existence of the Earth's eigen dipole magnetic field. In a recent observation by the Cluster spacecraft, EMIC triggered emissions were discovered in the inner magnetosphere. We further modified the hybrid code to incorporate a cylindrical geometry of magnetic field modeling the inner magnetosphere to reproduce the EMIC triggered emissions and analyze the nonlinear wave particle interactions. We assume a parabolic magnetic field to model the dipole magnetic field in the equatorial region of the inner magnetosphere. As shown in Fig. 2, we reproduce rising tone emissions in the simulation space, finding a good agreement with the nonlinear wave growth theory. In the energetic proton velocity distribution we find formation of a proton hole, which is assumed in the theory. A substantial amount of the energetic protons are scattered into the loss cone, while some of the resonant protons are accelerated to higher pitch angles, forming a pancake velocity distribution.

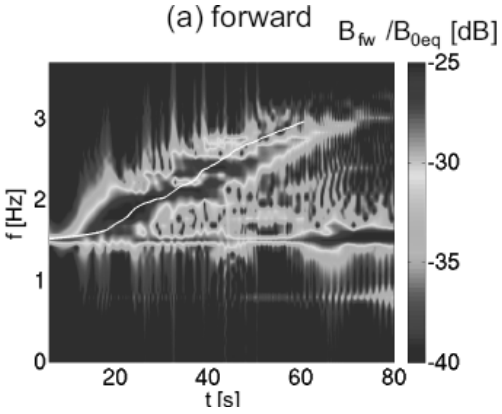

Fig. 2: Dynamic spectra of EMIC triggered emission.

Another type of EMIC wave with a constant frequency is occasionally observed below the He^+ cyclotron frequency after the multiple EMIC triggered emissions. In the presence of energetic protons with a sufficient density and temperature anisotropy, multiple EMIC triggered emissions are reproduced due to the nonlinear wave growth mechanism of rising-tone chorus emissions, and a constant frequency wave in the He^+ EMIC branch is subsequently generated. Through interaction with the multiple EMIC rising-tone emissions, the velocity distribution function of the energetic protons is strongly modified. Because of the pitch angle scattering of the protons, the gradient of the distribution in velocity phase space is enhanced along the diffusion curve of the He^+ branch wave, resulting in the linear growth of the EMIC wave in the He^+ branch.

Acknowledgments

Computation in the present study was performed with the KDK system of Research Institute for Sustainable Humanosphere (RISH) and Academic Center for Computing and Media Studies at Kyoto University as a collaborative research project. The present study was supported in part by a Grant-in-Aid for Research Fellows from the Japan Society for the Promotion of Science (JSPS).

References

[1] Shoji, M., Y. Omura, and L. C. Lee (2011a), Multi Dimensional Nonlinear Mirrormode Structures in the Earth's Magnetosheath, *J. Geophys. Res. in press.*

[2] Shoji, M., Y. Omura, B. Grison, J. Pickett, and I. Dandouras (2011b), Electromagnetic Ion Cyclotron Waves in Helium Branch Induced by Multiple Electromagnetic Ion Cyclotron Triggered Emissions, *Geophys. Res. Lett., 38,* L17102.

[3] Shoji, M., and Y. Omura (2011c), Simulation of electromagnetic ion cyclotron triggered emissions in the Earth's inner magnetosphere, *J. Geophys. Res., 116*, A05212.

[4] Shoji, M., Y. Omura, B. T. Tsurutani, O. P. Verkhoglyadova, and B. Lembege (2009), Mirror instability and L-mode electromagnetic ion cyclotron instability: Competition in the Earth's magnetosheath, *J. Geophys. Res., 114*, A10203.

ABSTRACTS (MASTER THESIS)

The characteristic of enzymatic saccharification on Cellulosic Biomass by ethylenediamine swelling treatment

**(Graduate School of Agriculture,
Laboratory of Biomass Morphogenesis and Information, RISH, Kyoto University)**

Naoya Konakahara

As sustainable resources for bioethanol production, cellulosic biomass has been receiving increasing interests. However, the effective pretreatment that allows stable and rigid structure of cellulose to be digested is still a major key target of intensive studies.

In this work, we studied the effect of ethylenediamine (EDA) treatment on the enzymatic hydrolysis of cellulosic biomass. This treatment induced intracrystalline swelling of cellulose I into III_I and morphological change such as fibrillation. The effect of EDA treatment on highly crystalline cellulose microfibrl as well as woody biomass was investigated.

Experiment

(1) The treatment on *Valonia ventricosa*

V. ventricosa film known as highly crystalline cellulose, was used as a standard sample. Purified cellulose was swollen into 100% EDA solution for 15min, successively washed by 100% methanol baths for 15 min. Repeating the whole procedures at ten times (EDA treatment), cellulose I_α was almost completely transformed into cellulose III_I. In addition, the transformation of cellulose I into cellulose III_I has been known to be a reversible reaction. Therefore, reproduced cellulose I_β was prepared by hydrothermal treatment (150℃). The crystalline polymorphs were confirmed by FT-IR ATR, then, these samples were incubated with a commercial cocktail named Accellerase 1500 (Genencor, Danisco US, Inc. Rochester, NY) for enzymatic saccharification.

(2) The treatment on Sugi

Thin longitudinal slices from wood block were treated Schultze solution at 60 ºC for 2 h under continuous stirring. The products were then thoroughly washed with distilled water until neutrality. The EDA treatment for Sugi was performed as mentioned above. In order to investigate the morphological change, Sugi was delignified by Schulze solution and its tracheid was isolated. After EDA treatment, the sample was observed by optical microscopy.

Results

(1) The effect of EDA treatment on *V. ventricosa*

The enzymatic hydrolysis of cellulose III_I (the sample treated by EDA treatment) proceeded much faster than that of cellulose I_α (the sample untreated by EDA treatment). As a result, saccharification ratio of cellulose III_I was reached 95% at 24h and increased 45% compared with cellulose I_α. Moreover, the saccharification ratio of regenerated cellulose I_β increased 16%, compared with cellulose I_α. This improvement is probably due to the effect of fibrillation of cellulose microfibril. The results obtained demonstrated that crystalline conversion from I into III_I clearly contributed to higher enzymatic saccharification than fibrillation.

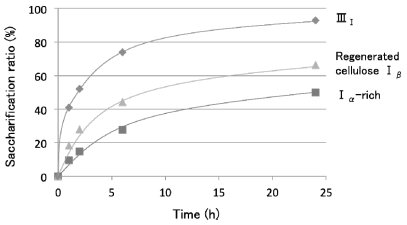

Figure Saccharification ratio of cellulose crystalline forms using *V. ventricosa*.

(2) The effect of EDA treatment on sugi

Although the crystal transformation by EDA treatment did not take place, the enzymatic saccharification ratio was improved. EDA treatment after maceration induce, the ballooning of tracheid observable under optical microscopy, which increased the internal surface area resulting in higher susceptibility to the saccharification.

Acknowledgements

The author appreciates Prof. Takashi Watanabe and Assistant Prof. Kentaro Abe (RISH, Kyoto University) for supporting HPLC systems and X-ray diffractometer.

ABSTRACTS (MASTER THESIS)

Quantitative analysis of cellulose synthase activity

**(Graduate School of Agriculture,
Laboratory of Biomass Morphogenesis and Information, RISH, Kyoto University)**

Kenji Shimono

Cellulose is one of the major biomass on the earth, and billions ton of that is produced a year by many biological organisms. This is because cellulose has been in general quite beneficial for those organisms by virtue of strong mechanical strength and biological resistance, which are given by its high crystalline fibrous structure with hydrogen bonding network, microfibril. The gene of cellulose synthase is identified in many species, and molecular and cell biological aspects of cellulose synthase is well understood. On the other hand, its enzymatic mechanism is just partially understood, and there are a lot of questions to be answered. Quantitative description of cellulose-synthesizing activity, for example enzyme kinetics, is very important for this purpose, and in my thesis, cellulose-synthesizing activity of a vinegar-producing bacterium *Gluconacetobacter xylinus* is quantitatively analyzed in vitro.

Experiments

Gluconacetobacter xylinus ATCC53524 was grown in SH-medium at 28°C until OD_{660} reaches to 0.5-0.7. Cells were ruptured by French-Press at 20,000 psi and then ultracentrifuged by 100,000g for 1 h to collect cell membrane fraction. Crude enzyme was solubilized from cell membrane by several detergents and the cellulose-synthesizing activity was measured with the ^{14}C-labeled substrate, UDP-D-[U-^{14}C]-glucose: the amount of ^{14}C incorporated into cellulose (ethanol insoluble fraction) was measured by liquid-scintillation counting. The specific activity was calculated and plotted as a function of substrate concentration to figure out substrate-saturation curve (S-V curve).

Results and Discussion

More than 30 conditions of solubilization (detergent molecule and its concentration) were tried and the synthesizing activity in detergent-extract was measured for 1h of reaction (Figure 1). It is noticeable that alkylmaltoside gave substantial activity in the extract. This type of detergent is one of the most successful ones in structural biology of membrane protein, implying less unfavorable interferes with protein. However, the activity in the extract is higher than that of cell membrane before solubilization, indicating activation of the enzyme by solubilization. Thus the enzyme might be substantially modified, and it is quite consistent with that this in vitro reaction produces cellulose II [1], a non-native form of cellulose. It will be supposed that cellulose synthase must be embedded in cell membrane for synthesizing cellulose I microfibril.

Using this protocol for counting the activity, kinetic analysis was carried out with the initial rate of the extract of decyl-β-maltoside. The concentration dependency of the activity about UDP-glucose and c-di-GMP was analyzed. As shown previously, c-di-GMP shows sigmoid S-V curve, indicating that the binding of c-di-GMP is cooperative about cellulose synthesis. Interestingly, S-V curve of UDP-glucose also shows sigmoidal feature in detergent extract, whereas it is hyperbolic before solubilization. K_m for UDP-glucose is 10^{-3} M while c-di-GMP has 10^{-6} M, and they do not change before and after solubilization. Although careful interpretation is necessary, these observations are very insightful.

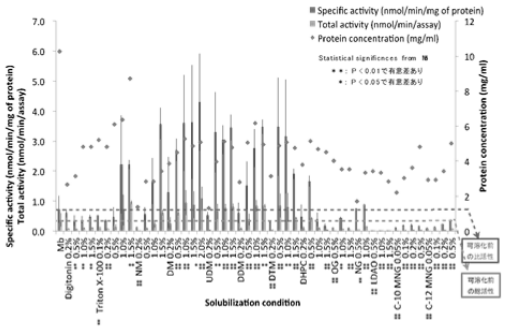

Figure 1 Total activity (green bars) and specific activity (red bars) of detergent-extracts. * and ** stands for significant difference from membrane (Mb) with $p<0.05$ and $p<0.01$, respectively.

References

[1] Hashimoto, A.; Shimono, K.; Ichikawa, T.; Horikawa, Y.; Wada, M.; Imai, T; Sugiyama, J. *Carbohydr. Res.* vol. 346, pp.2760-2768, 2011.

ABSTRACTS (MASTER THESIS)

Transcriptional response of a selective white-rot fungus to a lignin fragment

**(Graduate School of Agriculture,
Laboratory of Biomass Conversion, RISH, Kyoto University)**

Kenichiro Mori

White rot fungi are the only microorganism in nature that can mineralize lignin in wood. Some of fragments generated during lignin degradation are putative signal molecules that regulate the mechanism of wood decay. In a model species of white-rot fungus, *Phanerochaete chrysosporium*, its cellular response to vanillin, has been analyzed in detail [1]. Vanillin is one of the key intermediates found during lignin biodegradation. *P. chrysosporium* exposed to vanillin drastically changes the metabolic flux from the glyoxylate cycle to the tricarboxylic acid cycle and then activates the heme biosynthesis pathway.

On the other hand, a white-rot fungus, *Ceriporiopsis subvermispora*, has very different characteristics from *P. chrysosporium*: i) selective ligninolysis without serious damage to cellulose; ii) secretion of large amounts of fatty acids and their peroxidation at an early stage of wood decay; iii) high resistance to growth inhibition by vanillin; iv) no activity of lignin peroxidase; v) possession of a suppression mechanism of cellulolytic hydroxyl radical; vi) no activity of cellobiohydrolase.

In this study, the author focuses on cellular response of *C. subvermispora* to vanillin, and tried to analyze genes that were up-regulated by exogenous addition of vanillin.

Reference

[1] Shimizu, M., Yuda, N., Nakamura, T., Tanaka, H., and Wariishi. (2005) Metabolic regulation at the tricarboxylic acid and glyoxylate cycles of the lignin-degrading basidiomycete *Phanerochaete chrysosporium* against exogenous addition of vanillin. *Proteomics* **5,** 3919-3931.

ABSTRACTS (MASTER THESIS)

Structural analysis of secreted glycolipids by white-rot fungus

**(Graduate School of Agriculture,
Laboratory of Biomass Conversion, RISH, Kyoto University)**

Daisuke, Yamaguchi

Continued usage of fossil fuels has caused depleted energy problems and serious environmental issues such as global warming. Therefore, production of energy and chemicals from the most abundant renewable resources, woody biomass is an urgent task for ensuring sustainability of our life. In biological conversion of woody biomass, selective lignin degradation is a key process because cell wall polysaccharides in wood are surrounded by lignin. In nature, the degradation of lignin in wood occurs primarily through the action of lignin-degrading basidiomycetes called white rot fungi; consequently, this ecological group has received a considerable amount of research attention. Most of white rot fungi simultaneously decompose lignin and cellulose, accompanied by erosion of wood cell walls, while some fungi called selective white rot fungi, such as *Ceriporiopsis subvermispora* are able to degrade lignin without intensive damage of cellulose. Thus, a white rot fungus *C. subvermispora* is useful for the production of bioethanol, biomethane, pulp and feed for ruminant animals due to its selective lignin-degrading ability. This fungus secretes hydrophobic metabolites such as fatty acids and alk(en)ylitaconic acids (ceripiric acids). These metabolites play important roles in the selective lignin-degrading system. In this study, secreted glycolipids of the fungus were analyzed. At least two kinds of glycolipids were detected by thin layer chromatography with specific color identification reagent. Detected glycolipids were purified by high performance liquid chromatography (HPLC) and analyzed by hybrid mass spectrometer, LCMS-IT-TOF. Monosaccharide and aglycon moieties of the glycolipids were analyzed by MS^n fragmentation data of ESI-MS with high mass accuracy. After acid hydrolysis followed by extraction and derivatisation, we analyzed the monosaccharide and aglycon moieties of the glycolipids using GC-MS. The secreted glycolipids can be distinguished from those bound in cell membrane, and attract a great deal of interest in their functions in wood decay.

ABSTRACTS (MASTER THESIS)

Effects of copper on oxalate biosynthesis in the brown-rot fungus *Fomitopsis palustris*

(Graduate School of Agriculture, Laboratory of Metabolic Science of Forest Plants and Microorganisms, RISH, Kyoto University)

Hiromichi Hisamori

Wood-rotting basidiomycetes cause severe damage on wooden structures. To protect the wooden structures from the wood-rotting fungi, copper-containing wood preservatives have been used. However, many species of wood-rotting brown-rot fungi can degrade even the wood materials treated with the copper-containing preservatives, by which these wood-rotting fungi are called copper-tolerant fungi. The copper-tolerant ability has been recognized as being associated primarily with oxalic acid excretion, in which oxalic acid produced by copper-tolerant fungi reacts with copper in wood to form insoluble, bio-unavailable inert forms.

From a viewpoint of wood protection from the fungal degradation, the copper-tolerance of these wood-rotting fungi should be diminished. At the same time, the copper-tolerant wood-rotting fungi are promising to be used for bioremediation of wastes of woods treated with copper-containing preservatives [1]. Therefore, it is important to elucidate effects of copper on oxalate biosynthesis to develop bioremediation of copper from wood waste containing wood preservatives including copper.

Brown-rot fungus *Fomitopsis palustris* possesses two metabolic pathways for oxalate biosynthesis: one is hydrolysis of oxaloacetate catalyzed by oxaloacetate acetylhydrolase (*Fomitopsis palustris* oxaloacetate acetylhydrolase, FpOAH) in cytosol and the other is dehydrogenation of glyoxylate catalyzed by cytochrome *c* dependent glyoxylate dehydrogenase (*Fomitopsis palustris* glyoxylate dehydrogenase, FpGLOXDH) in peroxisome [2-4].

This author investigated effects of Cu^{2+} on oxalate biosynthesis including expressions of *FpOAH* and *FpGLOXDH*. In the absence of Cu^{2+}, amounts of *FpOAH* transcripts were 22 – 140 times greater than those of *FpGLOXDH*. The results suggest that FpOAH plays the more significant role than FpGLOXDH and the pathway including FpOAH as a key enzyme is a major pathway for oxalate biosynthesis, supporting our proposed idea that oxalate is biosynthesized mainly in the cytosol by FpOAH but not in the peroxisome by FpGLOXDH [2-4]. On the other hand, under the condition in the presence of Cu^{2+} an amount of *FpOAH* transcript was 19.4 times greater on day 4 (minimal magnitude) and 151.1 times greater on day 9 (maximal magnitude) than those of *FpGLOXDH*. The results suggest that FpOAH also plays a major role in oxalate biosynthesis regardless of absence or presence of Cu^{2+}.

However, the amounts of *FpOAH* and *FpGLOXDH* transcripts increased 2.2 and 7 times as their maximal rates by the presence of Cu^{2+}. The results indicate that Cu^{2+} increased expressions of *FpOAH* and *FpGLOXDH*, but the rates of the increments are suggested to be just several times.

References

[1] Kartal, S., and Imamura, Y. (2003) "Chemical and biological remediation of CCA-treated waste wood", *Wood Research* 90, 111-115.

[2] Munir, E., Yoon, J. J., Tokimatsu, T., Hattori, T., and Shimada, M. (2001) "A physiological role for oxalic acid biosynthesis in the wood-rotting basidiomycete *Fomitopsis palustris*", *PNAS* 98:11126-11130.

[3] Hattori, T., Okawa, K., Fujimura, M., Mizoguchi, M., Watanabe, T., Tokimatsu, T., Inui, H., Baba, K., Suzuki, S., Umezawa, T., and Shimda, M. (2007) "Subcellular localization of the oxalic acid-producing enzyme, cytochrome *c*-dependent glyoxylate dehydrogenase in brown-rot fungus *Fomitopsis palustris*", *Cellullose Chemistry and Technology*, 41: 545-553.

[4] Sakai, S., Nishide, T., Munir, E., Baba, K., Inui, H., Nakano, Y., Hattori, T. and Shimada. M. (2006) "Subcellular localization of glyoxylate cycle key enzymes involved in oxalate biosynthesis of wood-destroying basidiomycete *Fomitopsis palustris* grown on glucose", *Microbiology*, 152: 1857-1866.

ABSTRACTS (MASTER THESIS)

Characterization of lignocellulose in *Erianthus ravennae*

(Graduate School of Agriculture, Laboratory of Metabolic Science of Forest Plants and Microorganisms, RISH, Kyoto University)

Yuichiro Otake

Erianthus spp., an energy-producing plant, belongs to the tribe Andropogoneae, under the grass family Gramineae. Members of this genus are perennial grasses and are used worldwide as breeding material for sugarcane, a close relative. *Erianthus* spp. show better growth even under unfavorable environmental conditions, such as submersion, acidic soil, and dry-season soil drought. In addition, *Erianthus* spp. yield huge amounts of biomass; the yearly dry-matter yield is in the range of 40 to 60 ton ha^{-1} yr^{-1}. For these reasons, *Erianthus* spp. are receiving much attention as a potential biofuel and industrial feedstock. Surprisingly, despite the importance of *Erianthus* spp. as feedstock, detailed chemical analyses of its cell-wall constituents have not been reported. In gramineous plants, it is known that enzymatic hydrolysis or saccharification of the cell wall was inhibited not only by lignin but also by ferulic acid esters, which cross-links lignin and polysaccharides. Moreover, the states of being of their compounds in the cell wall were varied among plant species and even among organs with single plant species. Therefore, to exploit the potential of *Erianthus* spp., we must analyze lignins and cell-wall linked *p*-hydroxycinnamic acids including ferulic acid. In this study, *Erianthus ravennae*, a hardy *Erianthus* species originated from Mediterranean region and southwest and east Bulgaria that can be cultivated in Japan, was selected as a plant material, and especially the stem of *E. ravennae* was analyzed. The inner and outer parts of the *E. ravennae* stem differed distinctly in specific gravity and apparent hardness: the outer part was highly dense and very hard compared to the inner part. Thus, the author characterized the lignocellulose components and examined the enzymatic saccharification efficiency in the inner part and outer part of each internode of *E. ravennae* and profiled the variation among internodes and variation within a single internode.

Lignin contents of different internodes were 18.4–27.3 % in outer part and 17.1–24.5% in inner part. In addition, lignin aromatic components (S/V ratios) ranged from 0.63 to 1.13, and 0.43 to 0.96 in outer part and inner part, respectively. Lignin contents and S/V ratios roughly increased from top to bottom internodes. The amount of ferulic acid in both outer and inner parts slightly increased from bottom to top internodes, while that of *p*-coumaric acid had no tendency. Enzymatic saccharification efficiencies were 2.8–30.9% in outer parts and 17.5–38.6% in inner part, and increased from bottom to top internodes. Correlation analysis indicated that outer part of internodes showed a negative relationship between lignin content and enzymatic saccharification efficiency, whereas inner part did not. It indicates that there should be other factors that impede enzymatic saccharification than lignin content in inner parts. This is a new finding about lignocellulose components. The elucidation of the supramolecular structure of lignocelluloses in *E. ravennae* requires further studies including analysis of ferulate dimers crosslinking between carbohydrates.

The data of characteristics of lignin and related components in each internode of *E. ravennae* is helpful to further studies of *E. ravennae* aiming to improve the efficiency of lignocellulose utilization. Pretreatment such as alkaline treatment would be effective for the part with low saccharification efficiency. In addition, energy gaining from the parts with high lignin contents by direct burning should be considered to maximize the energy output/input balance. Taken together, the information obtained in the present study will help us to understand comprehensively the lignocellulose supramolecular structure and to improve the efficiency of lignocellulose utilization from grass plants.

ABSTRACTS (MASTER THESIS)

A comprehensive analysis of the changes in organic acid metabolism of ectomycorrhizal fungus *Laccaria bicolor* in response to aluminum salts

(Graduate School of Agriculture, Laboratory of Metabolic Science of Forest Plants and Microorganisms, RISH, Kyoto University)

Takaomi Ozasa

Ectomycorrhizal (ECM) fungi are a symbiont forming ectomycorrhizae on the roots of woody plants. The ectomycorrhizae play an important role for the woody plants in taking up water and nutrients such as nitrogen, phosphorus and minerals from soil through extrametrical ECM hyphae distributed widely in soil. Of the world's land surface where the agriculture is possible, 41.7% is classified as acid soils [1]. Due to acid rains, soil acidification is accelerated. By the mineral acid precipitation, aluminum is mobilized as Al^{3+} from rock containing minerals. In these acid soil areas, the Al^{3+} causes forest deterioration through inhibition of growth of plant roots, which is recognized as an Al-toxicity. However, several experimental evidences *in vitro* have shown that ECM fungi protect their host plants from the Al-toxicity. In the protective effect of ECM fungi, formation of stable and lower toxic chelate complexes with Al^{3+} by organic acids such as malate, citrate, and oxalate released from ECM fungi is essential for detoxification of Al^{3+}.

On the other hand, aluminum phosphate ($AlPO_4$), a source of phosphorus nutrient for ECM fungi and woody plants, is difficult to be solubilized by mineral acid [2]. However, $AlPO_4$ is solubilized by organic acids with chelating activity [3], by which dihydrogen orthophosphate ion ($H_2PO_4^-$) or hydrogen orthophsphate ion (HPO_4^{2-}) depending on pH in soil are released. These forms of phosphate can be utilized by fungi and host plants.

Therefore, it is important to elucidate mechanisms for detoxification of Al^{3+} and solubilization of $AlPO_4$ by ECM fungi for sustainable forest management. To elucidate the mechanism, ECM fungus *Laccaria bicolor* 1283 was grown on MMN agar medium containing $AlPO_4$ or $AlCl_3$ and metabolites in glycolysis, pentose phosphate pathway and tricarboxylic acid cycle were analyzed by CE-MS. Organic acids with chelating ability pooled in mycelia or released to medium were also analyzed by GC-MS.

CE- and GC-MS analyses showed that the amounts of most metabolites pooled in mycelia were increased and those of oxalic acid and citric acid released to medium were also increased several times when the fungus cultured with $AlPO_4$. On the other hand, $AlCl_3$ did not affect significantly on the amounts of the organic acids pooled in mycelia and released in medium.

The results suggest that increments of the amounts of organic acid pooled in mycelia and released in medium are due to effects of $H_2PO_4^-$ and HPO_4^{2-}, but not Al^{3+}. The two phosphorus anions taken up by *L. bicolor* are suggested to accelerate the release of organic acids with chelating activity. The more released these organic acids would more detoxify Al^{3+} by formation of chelate complex, which accelerates detoxification of Al^{3+} required for healthy growth of woody plants in acid soils.

References

[1] Okagawa, N. (1984) "Global distribution of acid soils and their use (in Japanese)", In Acid soils and their agricultural use: Present status and the future in topics (Tanaka, A. Eds.), Hakuyu-sha, Tokyo, pp 21-49.

[2] Plassard, C., et al. (2011) "Diversity in phosphorus mobilization and uptake in ectomycorrhizal fungi", *Annals of Forest Science* 68: 33-43.

[3] Otani, T. and Ae, N. (2001) "Interspecific differences in the role of root exudates in phosphorus acquisition", In Plant Nutrient Acquisition (Ae, N., Arihara, J., Okada, K., Srinivasan, A. Eds.), Springer, Tokyo, Japan, pp 101-119.

ABSTRACTS (MASTER THESIS)

Molecular analysis of a transporter protein ALMT in *Lotus japonicus*

(Graduate School of Agriculture, Laboratory of Plant Gene Expression, RISH, Kyoto University)

Tomohiro Kan

Root nodule formed with root cells of legume plant and rhizobia is a nitrogen-fixation apparatus, in which carbon and nitrogen compounds are exchanged between two organisms as symbiosis. For the establishment of nodules, it is important that flavonoids are released from roots as signal molecules, and Nod factors are produced in response by rhizobium, which are then received by the host plant. However, a large portion of the mechanisms are still unknown how metabolites are transport between plant cells and bacteroids and which transporters are involved.

In this study, we focus on a transporter family, Aluminum-activated malate transporter(ALMT) in a model legume, *Lotus japonicus*. ALMT was first identified in wheat as being a malate transporter that mediated Al-dependent efflux of malate chelates from the roots and detoxified Al cation in the rhizosphere.[1)] More recently, it has been turned out that ALMTs are widely distributed in the plant kingdom. Adding to the Al-activated malate transporter conferring Al tolerance to plant cells, an Arabidopsis member AtALMT12 expressed in guard cell is involved in the stomatal movement by regulating the malate transport.[2)] During symbiotic nitrogen fixation, organic acid and ammonia are exchanged between the root cells of legumes and the bacteroids, which mostly use the malate as a carbon source to manage the carbon metabolism. This suggests that malate plays a pivotal role in the symbiotic nitrogen fixation, and thus it has been thought that there should be a malate transporter in the nodules. We have then analyzed ALMTs in *L. japonicus*, whether this transporter is involved in the establishment and function of nodules.

1) Sasaki, et al., (2004) Plant J., 37: 645 - 653.

2) Sasaki, et al., (2010) Plant Cell Physiol. 51: 354 - 365.

ABSTRACTS (MASTER THESIS)

Isolation of cDNAs encoding prenyltransferase for flavonoid from *Macaranga tanarius*

**(Graduate School of Agriculture,
Laboratory of Plant Gene Expression, RISH, Kyoto University)**

Ryo Shimizu

Prenylation of an aromatic compound is a critical step to diversify the chemical structures and biological activities of secondary metabolites, and this reaction step is also involved in the biosynthesis of important endogenous quinone compounds like coenzyme Q and plastoquinone. The diversification of aromatic compounds by prenylation is via differences in prenylation position on the aromatic ring, various lengths of prenyl chain, and further modifications of the prenyl moiety, e.g. cyclization and hydroxylation, resulting in the occurrence of more than 1,000 prenylated compounds in plants.[1)] This biosynthetic reaction represents the crucial coupling process of the shikimate or polyketide pathway providing an aromatic moiety and the isoprenoid pathway derived from the mevalonate or MEP (methyl erythritol phosphate) pathways, which provides the prenyl (isoprenoid) chain.[2)]

In particular prenylated flavonoids have been actively studied as they show various biological activities beneficial for human health. These compounds frequently occur in some limited plant families like Moraceae and Leguminosae, while some other plant families are also known to contain prenylated flavonoids depending on the genus. *Macaranga tanarius* (Euphorbiaceae) is a tropical tree grown in Okinawa in Japan, which is a source of propolis in Okinawa area. Okinawan propolis contains characteristic prenylflavonoids, which are are geranylated eryodictiol derivatives.

In this study we have found several candidate cDNAs coding for prenyltransferases from a cDNA library prepared from glandular trichomes of *M. tanarius* fruits. They contain three characteristic sequences, i. e., putative transit peptide at the N-terminus, D-rich motif conserved among Mg-dependent prenyltransferases, and membrane-spanning domain. We have tried to express them in yeast and detected the enzyme activity of prenyltransferase using eryodictiol as the flavonoid substrate.

1) Yazaki, et al., Phytochemistry, 70: 1739 – 1745, 2009
2) Akashi, et al., Plant Physiol. 149: 683 – 693, 2009

ABSTRACTS (MASTER THESIS)

Study of UV/Visible Raman Lidar Systems for Profiling of Water Vapor and Aerosols

(Graduate School of Informatics, Laboratory of Atmospheric Sensing and Diagnosis, RISH, Kyoto University)

Chikara Miyawaki

It is projected that localized extreme weather events could increase due to the effects of global warming, resulting in severe weather disasters, such as a torrential rain, floods, and so on. Meanwhile, the interaction of atmospheric aerosol particles with water vapor is related to cloud condensation nuclei activity. A demand is increasing for development of a continuous observation system of the atmospheric water vapor and aerosols in the lower troposphere. We study in this thesis a Raman lidar which can obtain an accurate height profile of these parameters. We operated a Raman lidar for visible bands under different weather conditions, then, we have newly developed a UV (ultra-violet) Raman lidar.

We carried out observations with the visible Raman lidar at Shigaraki MU observatory located in a forest region. We found that the particle scattering associated with the water vapor content increased in autumn and summer. The results suggest that measurement of the aerosol particle size is required with a lidar system on multi-wavelength in order to know aerosol hygroscopic properties quantitatively.

We have developed a UV Raman lidar that can be operated even in urban areas, where human eye safety must be ensured. The nominal ocular hazard distance of this UV laser is about 130 m, which is one order of magnitude smaller than that for a visible laser. We conducted observations with this UV Raman lidar at Uji in July 2011. The vertical resolution of the water vapor profile is 116m and 26m at an altitude of 1.0 km with an integration time of 300 s and 900 s, respectively, which is estimated from the statistical uncertainty resulting from signal noise. We found, however, some optical detection components of the lidar system are sensitive to ambient temperature, and the detected signals fluctuated periodically because of room temperature variations. Therefore, we smeared out the periodic variations, which degraded the time resolution to 1800 s from the implicit resolution. Employing both UV and visible Raman lidars, we studied aerosol hygroscopic processes and clarified particle growth with the increase in water vapor content.

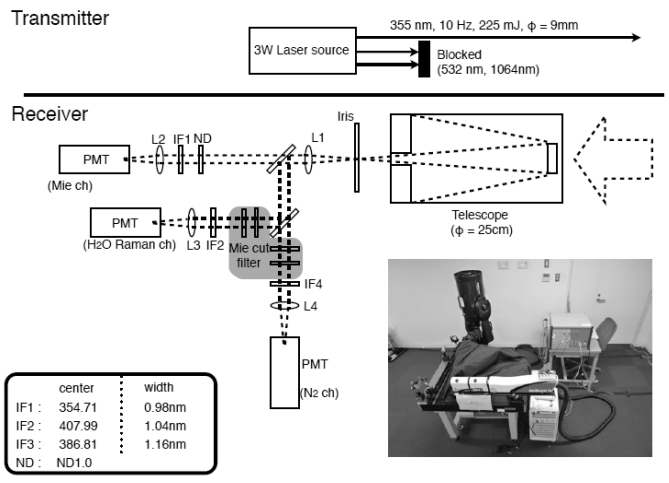

Figure 1. A schematic of the developed UV Raman Lidar system

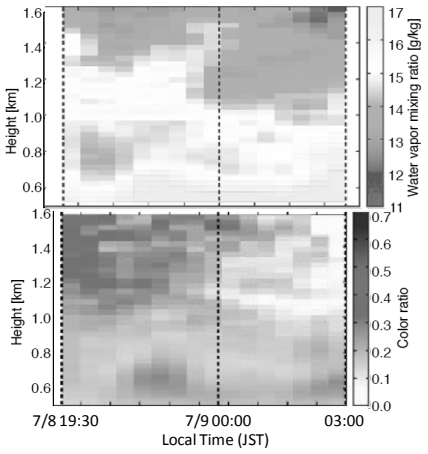

Figure 2. Water vapor mixing ration (top) and aerosol color ratio (bottom) from the UV Raman Lidar at Uji, Kyoto, for July 8-9, 2011. The color ratio, which here is the ratio of backscatter coefficients at wavelength of 532 and 355 nm, gives a measure of effective particle radius.

ABSTRACTS (MASTER THESIS)

Interannual variability in the seasonal evolution of the stratospheric circulation in the southern hemisphere

(Graduate School of Science, Laboratory of Atmospheric Environment Information Analysis, RISH, Kyoto University)

Shinya Nino

In the winter polar stratosphere there exists a strong cyclonic circulation, called the polar vortex, with cold temperatures. In the southern hemisphere, the polar vortex is stronger than in the northern hemisphere, and consequently it lasts long until November or December. During the transition period from winter to summer around September to November, zonal wavenumber 1 anomalies in the meteorological fields are dominated at high latitudes. It is reported by Hitchman and Rogal (2010) that the wavenumber 1 anomalies in temperature move eastward along with the seasonal evolution. Moreover, Hassler et al. (2011) pointed out that the phase of temperature anomalies in October tends to locate eastward year by year. Thus, the phase of temperature anomalies in the southern hemisphere stratosphere moves eastward from the view point of the seasonal evolution and the year-to-year variation, but previous studies only focused on the seasonal variation in climatologically averaged fields or on the year-to-year variation at the fixed time of the seasonal evolution in the southern hemisphere. In this study, using the reanalysis meteorological data for the period of 1957 to 2010, we made analyses on the wavenumber 1 temperature anomalies during the transition from winter to summer to grasp the characteristics of the seasonal evolution and its year-to-year variability. Based on the results about the eastward movement seen in the seasonal evolution and in the year-to-year variability, we try to propose that the seasonal evolution from winter to summer could be getting earlier in the southern hemisphere stratosphere.

First we investigated the zonal temperature anomalies along the seasonal evolution. In addition to the eastward movement of the phase shown by Hitchman and Rogal (2010), the latitude where the temperature anomaly is maximum moves poleward. Consequently, the temperature anomalies move eastward and poleward as the season goes by. Next we investigated the year-to-year variability in the phase and amplitude of the temperature anomalies. We found that the latitude where the temperature anomaly is maximum moves poleward in the seasonal evolution from September to October. During this period the amplitude of the wavenumber 1 temperature anomalies tends to become large, suggesting that planetary wave activity becomes vigorous. The year-to-year variability in the poleward movement of maximum temperature anomalies is similar to that seen in the seasonal evolution from September to November. These results suggest that the structure of the zonal temperature anomalies in October is getting close to that in November; in other words, the seasonal evolution of the stratospheric circulation in the southern hemisphere is getting earlier.

We further investigated the year-to-year variability in the total ozone field. The phase relation between the temperature and total ozone fields show clear relation with a correlation coefficient over 0.9. This indicates that enriched ozone and higher temperature could be observed coincidentally because of the stranger downward motion. Up to recent years it has been observed that the polar ozone is decreasing, so it is suggested that resulting cooling by ozone decrease may speed up the seasonal evolution during the transition period from winter to summer in the southern hemisphere.

References

[1] Hitchman, M. H., and M. J. Rogal (2010), *J. Geophys. Res.*, 115, D20104, doi:10.1029/2009JD012844.

[2] Hassler, B., G. E. Bodeker, S. Solomon and P. J. Young (2011), *Geophys. Res Lett.*, 38, L01805, doi:10.1029/2010GL045542, 2011

ABSTRACTS (MASTER THESIS)

An analysis on the variation in low clouds over the subtropical ocean using satellite data

(Graduate School of Science, Laboratory of Atmospheric Environment Information Analysis, RISH, Kyoto University)

Tota Yamada

Clouds strongly contribute to the earth's radiation budget. In particular radiative forcing of low clouds is large and it is about 60% of the total net radiative forcing averaged over the globe (Hartmann et al., 1992). Therefore it is important to investigate the variation of low clouds in terms of the earth's climate. It is known that low clouds mostly occur where the sea surface temperature (SST) is low, then Klein and Hartmann (1993) found a positive correlation between the seasonal evolutions of low cloud amounts observed from ship in the subtropical ocean and those in lower-tropospheric stability (LTS). Moreover, Wood and Bretherton (2006) proposed a use of estimated inversion strength (EIS) that was an improved measure of LTS, and found that the correlation between low cloud amounts and EIS is good even over the mid-latitude ocean. As the dataset they used consists of three-month mean climatologies of low cloud amounts, they only discussed about the seasonal variation, but not about the interannual variation. On the other hand, satellite cloud data have been used for the analyses of low cloud variations recently, but they are mostly concentrated on specific areas. In this study we use monthly mean cloud data from the satellite observations to investigate characteristics in seasonal and interannual variations of low cloud, EIS, and SST over the following 5 areas, off-shores of Peru, Namibia, California, west Australia, and Canary Islands.

First the seasonal variations for the five areas are investigated. Except the offshore area of the western Australia, we found high correlations between EIS and low cloud amounts, supporting the previous studies. The offshore area of the western Australia is assumed that horizontal advection should be taken into account for the understanding of variations in low cloud amounts over this area, because there are fair amounts of low cloud such as fog at high latitudes. Also the relation between SST and EIS is different in each of the five areas; the offshore areas of Peru and Namibia show very strong correlations, those of California and west Australia do not show clear correlations, and that of Canary Islands shows a slight correlation. These correlations suggest that EIS could be affected by temperatures at different height range, thus we need to pay attention to the vertical structure of EIS in detail.

Next we look at the interannual variability of low cloud amounts for each season averaged over three months. In the areas where the seasonal correlation between EIS and low cloud amounts is high, we found high correlations in interannual variations between EIS and low cloud amounts during the season when the variability of low cloud amounts is largest. Contrarily, in the areas where the seasonal correlation between SST and EIS is high, we found lowest correlations in interannual variations of SST and EIS during the season when the variability of SST is largest. Moreover, it could be expected that there may exist interannual variability in low cloud amounts and EIS in relation to the El-Nino and La-Nina cycle over the offshore areas of Peru and California, but it was not clearly seen. This is also the case for the area where the SST variations in association with the El-Nino and La-Nina cycle is evident at low latitudes.

References

[1] Hartmann, D. L., M. E. Ockert-Bell, and M. L. Michelsen (1992), *J. Climate*, 5, 1281-1304.

[2] Klein, S. A., and D. L. Hartmann (1993), *J. Climate*, 6, 1587-1606.

[3] Wood, R., and C. S. Bretherton (2006), *J. Climate*, 19, 6425-6432.

ABSTRACTS (MASTER THESIS)

Reinforcement effect of surface chemically modified cellulose nanofibers in natural rubber

(Graduate School of Agriculture, Laboratory of Active Bio-based Materials, RISH, Kyoto University)

Hayato Kato

Introduction

As a new material featuring light weight, high strength, and low thermal expansion, cellulose nanofibers (CNF, width: 15 nm – 20 nm) are expected to use as nano-fillers for resins, elastomers, and so on. However, CNF has a poor affinity for hydrophobic polymers since CNF has a lot of hydroxyl groups. To attain high reinforcement effects of CNF as a filler, chemical treatments of CNF are inevitable. In this study, we investigated mechanical reinforcement of natural rubber (NR) by chemically modified CNF.

Experiments

CNF was prepared from bleached softwood pulp by using a grinder. Then, chemically modified CNF was obtained by the reaction with pyridine and acid chloride. Saturated fatty acid and unsaturated fatty acid were incorporated into CNF surface. Control CNF was mixed with natural rubber latex in water, whilst chemically modified CNF was mixed with natural rubber solution in toluene. After drying, sulfur cross-linking reaction (vulcanization) was performed. Then, tensile tests, scanning electron microscope observation of fractured surface, thermal analysis and so on were performed.

Results and discussion

In this report, we mainly explained the reinforcement effects about stearoyl CNF (stCNF), which has saturated side chain groups, and oleoyl CNF (oleCNF), which has unsaturated side chain groups, with equal carbon number (C18). Incorporation of stearoyl CNF 5 wt% increased Young's modulus of natural rubber from 1.7 MPa to 18.6 MPa, and reduced thermal expansion of natural rubber from 226.1 ppm/K to 36.3 ppm/K. These results are attributable to the improvement of dispersibility and affinity of CNF in natural rubber by chemical modification. Moreover, oleoyl CNF 5 wt% increased Young's modulus of natural rubber to 27.7 MPa, and reduced thermal expansion to 18.6 ppm/K. These significant reinforcement effects can be explained not only by the improvement of dispersibility and affinity of CNF but also the formation of the sulfur cross-linkage between natural rubber and CNFs.

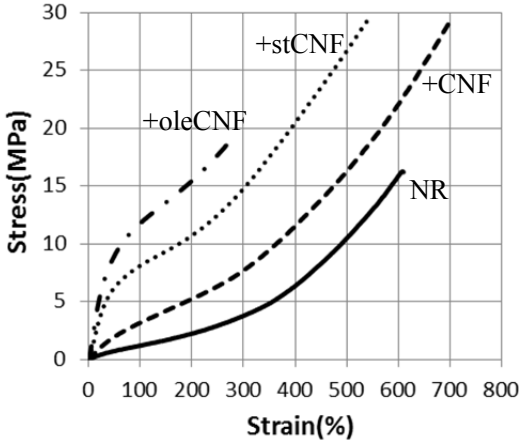

Fig.1 Stress-Strain Curves of natural rubber and CNF nanocomposites (CNF content: 5 wt%)

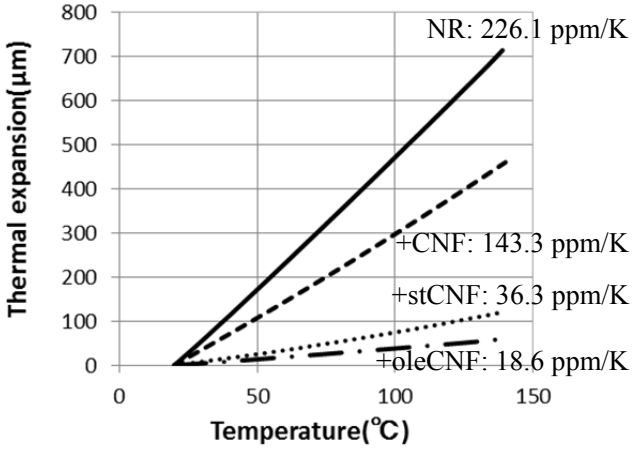

Fig.2 Thermal expansion of natural rubber and CNF nanocomposites (CNF content: 5 wt%)

ABSTRACTS (MASTER THESIS)

Clarification of NO_2 sorption behavior and Assessment of air quality in warehouse of cedar timber

(Graduate School of Agriculture, Laboratory of Sustainable materials, RISH, Kyoto University)

Miyuki Nakagawa

Introduction

In recent years Japanese cedar (*Cyptomeria japonica*) wood showed high NO_2 sorption ability compared with other wood species. The cross-sectional surface of tracheid, the extractives and the moisture of wood were the factors affecting the sorption performance of NO_2. However, the influences of these factors are not evaluated in detail. Japanese cedar timber also showed high humidity control function in end grain. As a material the flat-sawan Japanese cedar timber slitted across the end grain is developer. However, there were few evaluation studies in actual space. This research discusses the characterization of the NO_2 sorption behavior with various sample configurations and drying methods and the humidity-control function of Japanese cedar.

Methods

[1]NO_2 sorption behavior: In an incubator at 20˚C, samples of Japanese cedar with various configurations and drying method were aerated with an air under the NO_2 concentration of 1000ppb (low velocity: 560ml/min). NO_2 concentration before and after passing through the samples was monitored with a NOx analyzer for 24hrs. The amount of NO_2 sorption was calculated and compared among various samples.

[2]Humidity control function: In indoor warehouse cedar slitted panels were set, and the change of temperature and relative humidity, aldehyde concentration and metal corrosion were measured for a year.

Results and discussion

[1] Fig.1 shows the amount of NO_2 sorption of 1.5mm-thick discoidal and 15mm-thick plated specimens of cross-section where the gas flows through/over the tracheid, respectively. The former absorbed the NO_2 much more than the latter. This indicated that the effect of NO_2 sorption depends on available inner surface area of contact. NO_2 sorption ratio of the specimens decreased with the increase of drying temperature due to the amount of extractives in the specimen, thus the amount of NO_2 sorption is affected by the extractives of the specimens.

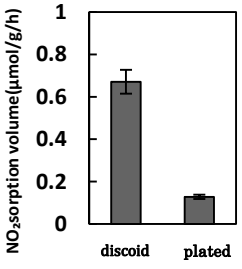

Fig1. NO_2 sorption volume of different gas contact condition

[2] The relationship between the amount of cedar slitted panels and humidity change ratio in air volume at indoor warehouse described a high correlation. It means that the cedar slitted panels have a high humidity control function in actual space.

ABSTRACTS (MASTER THESIS)

Development of Plywood Bonded with Citric Acid.

**(Graduate School of Agriculture,
Laboratory of Sustainable materials, RISH, Kyoto University)**

Kensuke Nakura

Introduction

Recently, various kinds of synthetic resins derived from fossil resources are used as adhesives in the wood industry. However, fossil resources are not renewable and are being steadily exhausted. Furthermore, synthetic resins are not good for environment and human health. The development of the alternative adhesives made from non-fossil resources is required. In this study, plywoods using citric acid as a natural adhesive were made, and physical properties were investigated.

Materials and Methods

Japanese cedar veneer and citric acid were used in this research. The veneer (300mm×300mm×3mm) was rotary-cut veneer of sapwood made of Japanese cedar (MC=8~11%). Citric acid as adhesive was pulverized into powder (less than 250 μm). Saccharides and lignocellulose powders with the same size were used as additives. The powder was sprinkled on veneer surface, and 3-ply plywood was manufactured. The condition of citric acid content, press temperature, time, and pressure were adjusted to 20~200g/m^2, 180 to 240°C, 3 to 15 minutes, and 1MPa respectively. According to Japanese Agricultural Standard, dry bond strength test and repeated boiling test were performed to evaluate mechanical properties of plywood.

Results and discussion

Fig.1 shows the relationship between press temperature and bond strength of plywood. In the case of 180℃, the dry bond strength was low, and the wet bond strength was not obtained due to decomposition during treatment. However, the bond strength increased with increasing press temperature. When press temperature was 220℃, the bond strengths were 0.93MPa (Dry) and 0.57MPa (Wet). In case of at 240℃, the bond strengths were similar to those of at 220℃. This indicated that the press temperature of 220℃ is needed to get good bond strength.

Considering the results of other experiments, the suitable manufacture condition of plywood using citric acid was 220℃, 10 minute, 60g/m^2.

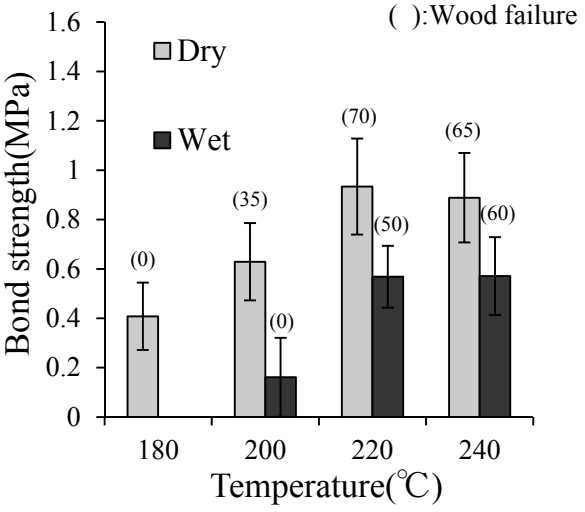

Fig1. Effect of press temperature on bond strength at 60g/m^2, 1MPa for 10 minutes.

ABSTRACTS (MASTER THESIS)

The evaluation of visual differences among variously dried woods - for the utilization of Japanese forest products -

(Graduate School of Agriculture, Laboratory of Structural Function, RISH, Kyoto University)

Mayu Ueda

Introduction

Now, Japanese forest has become mature and utilizable for timber. However, we encounter severe difficulties for utilization of them. One of them is confusions on the method of wood drying. Especially, Japanese cedar (Sugi: *Cryptomeria Japonica*), which is endemic to Japan has high moisture content and is difficult to dry. The kiln drying with high temperature is the most popular, but its dried products are bad visual condition because of burned surface. In this study, we evaluated the visual differences, color and gloss among variant dried-woods for improvement the dry technology and quality management.

Materials and methods

Sugi (135×135×4000mm) was used for specimen and cut into two members; 3000mm for kiln drying and another 1000mm for natural drying. Four different kiln drying methods were used such as high temperature drying, drying with high frequency wave, drying under decompression and medium temperature drying. The former three methods were subjected to high temperature steam process to control dimension change. 10 lumbers were provided for each kiln drying and 40 lumbers for natural drying. The specimens of 120×120×15mm were taken from these lumber for measuring of color and gross. Values of the color of the wood on the CIE*L *a*b**system was measured by imaging spectrophotometer (JFE Techno-Research Corporation) and gross was measured by a gross meter instrument (NIPPON DENSHOKU).

Results end discussion

Figure 1 shows the value of lightness *L** of sapwood color of each kiln dried samples and natural dried samples. The values of kiln dried were lower than that of natural dried. It is considered that the sapwood color became darker thorough kiln drying. The lightness of high temperature drying was lowest and that of high frequency wave was second lowest among kiln methods. Among kiln drying methods, three methods subjected to high temperature steam process showed significantly lower value in lightness. From this, it may be said that the drying schedule after this process mainly influenced on the lightness of sapwood. On the other hand, the value of redness *a** of heartwood showed different tendency. The value of above-mentioned three kiln methods was lower than that of natural, while medium temperature was not remarkably different from natural. In addition, the redness didn't show positive differences among above three kiln methods. From this, we may say that the redness became faint through high temperature steam process. In fact, the color change by kiln drying shows different behavior between sapwood and heartwood. The relation to high temperature steam process should be researched more particularly.

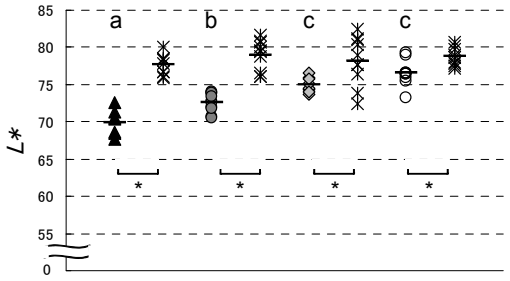

Figure 1. The Lightness difference of sapwood
Legend: ＊natural drying ○medium-temp drying
◆decompression ●high frequency wave
▲ high-temp drying ― average

ABSTRACTS (MASTER THESIS)

—Proposal of new reinforcing method on existing wooden traditional dwelling house without big change on superstructures.—

**(Graduate School of agriculture, Forest science dev.
Laboratory of Structural function, RISH, Kyoto University)**

Makiko (Miki) Yokozeki

How should we reinforce existing traditional wooden houses against earthquake without changing internal atmosphere of the building? It's not appropriate to add much amount of shear walls for reinforcement. In general, high performance shear wall needs the strong leg joints against pull-out force. But the columns in Japanese traditional timber structure are simply put on the stone base on the ground without metal joint. This makes it difficult to set high performance shear walls in such old timber structure. Thus we tried to invent a frame system to make shear walls work effectively by utilizing the space under the floor level in combination with less amount of shear wall.

1. Concept of reinforcement by frame system: The purpose of research is to develop the high performance shear wall and to reinforce existing timber frames. We developed a shear wall by combining lattice and board elements which satisfied the performance of high strength and deformation ability by taking the advantages of each element. This wall was set in the frame in which top and bottom beams were turned into boxed beam. Thus the pull-out force on the shear wall can be transmitted to the distant column by bending and shear resistance of the box beam and can be held down by smaller self load of the building.

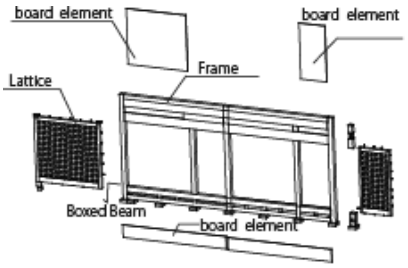

Figure 1. Outline of the frame system

2. Experimental: The height and width of the frame was almost 3015mm each as shown in Figure 2. The specimen consists of the hanged wall, the boxed beam with under the floor, shear wall and frame structure. Three types of shear wall, 1P, 2P and 1P×2 were set in the frame as parameters; here 1P wall means 1005mm in width. The each type of specimen was tested in 5 steps; gradually adding the structural elements such as lattice, board and top or bottom beam into the frame. The shear wall was composed by lattice made of Japanese cedar and the fibers mixed calcium silicate board nailed at each circumferences as well as at each intersection point of lattice members. We evaluated its mechanical properties by static horizontal cyclic loading test. The interaction of vertical and horizontal load was simulated by using wire-pulley system to give constant vertical force of 10, 20, 30kN while applying cyclic horizontal force by oil-jack.

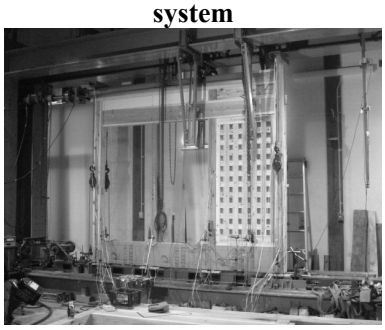

Figure 2. Test setup

3. Results and discussions: The maximum strength of the frame was about 30kN in condition over vertical load of 30kN as shown in Figure 3. The stress analysis showed the contribution of the only frame element was about 10kN. This high performance was achieved because the shear wall had enough strength as expected, and the whole frame structure worked well against the force in conjunction with hanged wall and boxed beam by virtue of the strong joints of the each part of the frame. The self-load sufficiently held specimen down against lifting up. In conclusion, we would say that it is possible for high performance shear wall to work effectively in the frame without leg joints by appropriately reinforcing the beams and joins. Based on the results, we adopted the system to reinforce a 200 years old timber building in traditional preservation district.

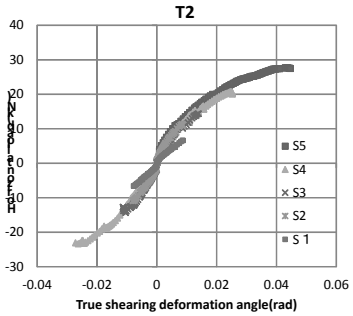

Figure 3. Load-deformation curves of test results.

ABSTRACTS (MASTER THESIS)

Effects of Diet Composition on Nutritional Physiology and Ecology of *Lyctus africanus* (Lesne)

**(Graduate School of Agriculture,
Laboratory of Innovative Humano-Habitability, RISH, Kyoto University)**

Titik Kartika

Several artificial diet combinations, wood- and non-wood-based, had been developed for *Lyctus brunneus*. It was reported that cellulose-based diet was more suitable for mass culture of *L. brunneus* than that of the wood particle (sawdust)-based one. This study discussed the probability of wood- and non-wood-based diets for *L. africanus* by examining the growth rate, oviposition ability and digestive enzyme (endoglucanase) activity of *L. africanus*.

Three diets, wood particle-based (WP), cellulose powder-based (CP) and alpha cellulose-based (AC) diets, were prepared, and then subjected to adults of *L. africanus*. Subsequent generations were used to examine the growth rate, population, body weight, and sex ratio (adult stage), oviposition ability (adult stage) and endoglucanase activity (larval stage).

The WP and CP diets generated equivalent growth rate of *L. africanus* with the similarities on average population, sex ratio (male/female) and body weight (Table 1). In the oviposition test, adult insects fed with CP- and AC-based diets tended to oviposit more eggs than that WP-fed adult did. In addition, the adults generated from the CP-based diet tended to survive longer after ovipositing the eggs (Fig.1). The endoglucanase activity was higher in CP- and WP-fed larvae than in AC-fed ones (Fig.2). These results implied that WP and CP diets might substitute each other to support growth of *L. africanus*.

Table 1. Growth rate of *L. africanus* on three diets

Diet sources	Population	Sex ratio (M/F)	Body weight (mg)
WP	206.000[a]	0.983[a]	1.983[a]
CP	188.875[a]	0.834[a]	1.866[a]
AC	55.875[b]	0.753[a]	1.966[a]

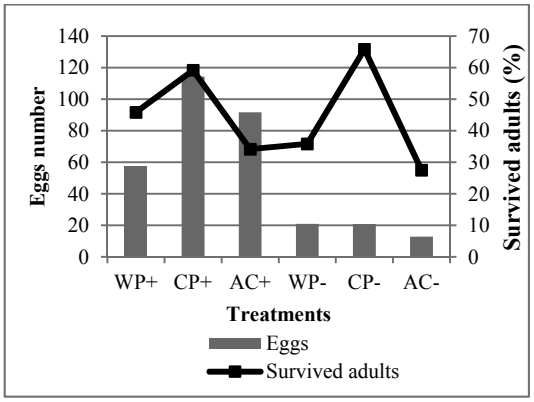

Fig 1. The number of eggs and survived adults of *L. africanus* after oviposition test

Note: (+) indicates the treatment of filter paper with nutritive solution; while (-) indicates the treatment of filter paper with water

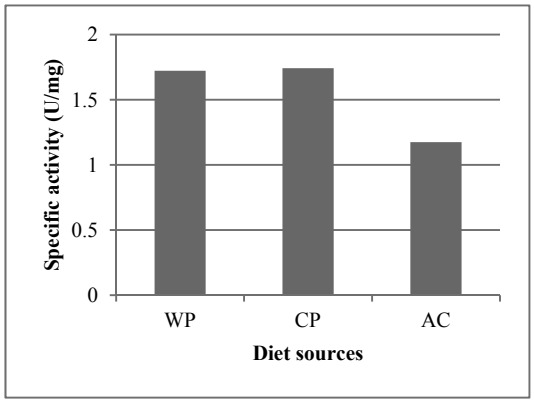

Fig. 2. Endoglucanase activites of *L. africanus* larvae fed with three different diets

ABSTRACTS (MASTER THESIS)

Development of carbonized cellulose as catalytic cathode in fuel cells

**(Graduate School of Agriculture,
Laboratory of Innovative Humano-Habitability, RISH, Kyoto University)**

Ryohei Asakura

Introduction

Research and development of environment-friendly energy is conducted worldwide. Fuel cells are significantly more energy efficient and cleaner than combustion-based power generation technology. Especially, polymer electrolyte fuel cells (PEFC) have attracted much attention in recent years as platinum applied as a catalytic electrode in PEFC is an extremely expensive precious metal. Therefore, the development of low-cost non-platinum catalyst is needed. One of the solutions is to use nitrogen-doped carbon as cathode material, which has been recognized as a promising root to enhance the electrocatalytic activity of carbon materials. Cellulose, from a renewable biomass resource, was used as a raw material in this study. Cellulose acetoacetate (CAA) was prepared in order to introduce metal ions such as Fe or Co into cellulose. In this study, cellulose acetoacetate prepared from microcrystalline cellulose was at first metal (Co,Fe) loaded then N-doped with melamine and the effects of the chemical and carbonization treatments on the chemical composition, microtexture and electrochemical performance of the materials were investigated.

Materials and Methods

Metal loaded CAA, prepared with diketene, mixed with melamine as nitrogen source was carbonized at 600-900ºC under N2 atmosphere by applying a pulse current sintering method, in which current is directed straight through the graphite dies as well as the sample, so that the sample was heated both from the inside and outside at the same time. This method can be considered to control pore size distribution by changing the heating rate which depends on the current applied to the sample. Surface chemistry of N-doped carbonized cellulose was investigated using X-ray photoelectron spectroscopy (XPS). The microstructure of the carbons was characterized by transmission electron microscopy (TEM) and N2 adsorption measurement. The ORR activity of the N-doped carbonized CAA particles was studied using the rotating disk electrode voltammetry.

Results and Discussion

BET specific surface area measurements on the sample with Co carbonized at 800°C resulted in 200m2/g and a shell-like nanostructure. The potential which was measured at the current density of -2μAcm-2 in the electrochemical measurement for N-doped carbons showed a clear dependence on sintering temperature. Graphitic nitrogen measured with XPS seemed to contribute to the improvement of the potential. Crystallization and the reaction of carbon with nitrogen seemed to have an important influence.

Conclusion

The present study shows that the catalytic action of transition metals during carbonization of CAA performed by pulse current sintering at different temperature and the nitrogen doping modify both the microtexture and the chemical composition of the carbonized material and consequently control the oxygen reduction reaction activity.

References

Asakura, R., T. Hata, Y. Uchimoto, R. Benoit, S. Bonnamy, P. Bronsveld, T. Yoshimura, "Carbonized cellulose as catalytic cathode in fuel cells," Proceedings of 1st International Symposium for Sustainable Humanosphere (ISSH2011), pp.55-52, 2011.

ABSTRACTS (MASTER THESIS)

Evaluation of trail-following and attracting activities of some chemicals against the dry-wood termite *Incisitermes minor*（Hagen)

**(Graduate School of Agriculture,
Laboratory of Innovative Humano-Habitability, RISH, Kyoto University)**

Emiria Chrysanti

1. Introduction

Information on termite's response toward chemicals such as trail pheromones and attractants could be valuable as a lure or bait for their control. However, this information is still limited simply to subterranean termites. The lack of information on chemical behavior of dry-wood termites is partially due to their feeding behavior: a single piece feeder. In this study, workers of the dry-wood termite, *Incisitermes minor* (Hagen) were investigated for their response to a trail pheromone candidate and several other possible attractants by trail-following and Y maze odor bioassays in combination with analysis of semiochemicals from alive termite and body extract.

2. Materials and Methods

Only workers were used in the bioassays. Chemicals used were a trail pheromone candidate (*Z*)-3-dodecenol, and possible attractants 2-phenoxyethanol, *d*-camphor, and maple lactone. The circular open-field bioassay was conducted with a Ø 12.5-cm filter paper. The termite was allowed to walk in Ø 7-cm pencil line (n=20). Parameters observed were number of individual with positive response (termite walk continuously in 3-cm line), distance travelled and walking speed. In the odor bioassay, a Y plastic maze (5-cm in both stem and branch length) was placed on a Ø 15-cm filter paper, and termite was allowed to choose between the chemicals and control (n=20). For semiochemical identification the body extracts of 60 workers were obtained by soaking into 600 µl hexane for 18 hours in room temperature. In the head space sampling, sixty workers were put into Monotrap (MT) kit and exposed to the absorbent MT RCC18 for 24 hours. The absorbent was then dipped into 70µl hexane, and sonicated for two minutes. All hexane samples were analyzed with a 5973N Mass Selective detector coupled to a 6890 Gas Chromatograph (Agilent Technologies, Palo Alto, CA).

3. Results and Discussion

In the trail-following bioassay, (*Z*)-3-dodecenol showed significantly positive responses for all concentrations in comparison with those of the control, but no significant response was observed in the odor bioassay. This finding confirms the previous report, indicating (*Z*)-3-dodecenol as a main component of trail pheromone from seven dry-wood termite species. In the attractant series, *d*-camphor showed the significant results both in the number of response and distance travelled for the circular open-field bioassay. Only 2-phenoxyethanol showed the significant result in number of positive individuals in the odor bioassay. This chemical has been reported as a trail-following mimic and attractant to subterranean termites. Dodecanol was identified from the *I. minor* body extract. The chemical was also reported in the dry-wood termite *Kalotermes flavicollis*. (*Z*)-3-dodecenol was not found in the present analysis probably due to different methods extraction. Nonanal and 2-nonanone were identified from the head space sample for the first time from termites.

ABSTRACTS (MASTER THESIS)

Evaluation of the nutritional requirement for the culture of a termite mushroom, *Termitomyces albuminosus* (Berk.) Heim

**(Graduate School of Agriculture,
Laboratory of Innovative Humano-habitability, RISH, Kyoto University)**

Kazuko Ono

Introduction

Termitomyces eurrhizus (Berk.) Heim is widely distributed in the tropical and subtropical region from Africa to Southeast Asia. This fungus is one of the termite mushrooms, living symbiotically in the fungus-garden of the nest of termites classified into Macrotermitinae. In Japan, *T. eurrhizus* is only found in Ishigaki Island, Iriomote Island and the limited area of Naha City of Okinawa's main Island, Okinawa Prefecture, in the presence of *Odontotermes formosanus* Shiraki.

Termite mushrooms are rare seasonal products, because they can only be harvested during a special period. To date, no artificial production of termite mushrooms have been accomplished mostly due to limited knowledge on their nutritional requirement.

In order to achieve artificial production of *T. eurrhizus*, strain-depending nutritional requirement of this species was evaluated in this study.

Materials and methods

Thirty-three strains of *T. eurrhizus* : 27 strains collected in Okinawa Prefecture, Japan (T1-22 and T24-28), 2 strains from American Type Culture Collection (ATCC) and 4 strains from National Institute of Technology and Evaluation's Biorogical Resource Center (NBRC) were obtained, and they were used for the first screening test. All strains were cultivated on 7 plate media at 26 °C in the dark, and mycelial growth was measured at 10, 15, 20, 25, 30, 35, 40, 45 and 50 days post inoculation. From the results of this screening, six strains were selected for the next experiments by their low specificity to the media and rapid mycelial growth.

The selected strains were cultivated on hay extract media with (HA-a) and without (HA-b) 0.2% (w/v) K_2HPO_4. These strains were also evaluated for their groeth on four Matsutake media, with different carbohydrate sources: glucose, sucrose, maltose and xylose. These strains were inoculated with 7 mm-diameter pre-cultured agar media, and the plates were incubated at 26 °C in the dark. Mycelial growth was measured at 10, 15, 20, 25, 30, 35, 40, 45 and 50 days post inoculation as well as the first screening test.

Results and discussion

There was no difference in mycelial growth of 6 strains between two HA media : HA-a with 0.2% K_2HPO_4 and HA-b without K_2HPO_4. This suggested that *T. eurrhizus* did not require any additional phosphate to grow on HA. *T. eurrhizus* may have low phosphate requirement.

When using Matsutake media with different carbohydrate sources, no difference in mycelial growth was observed for glucose, sucrose and maltose. On the other hand, the slower mycelial growth was obtained in the xylose-containing medium. Further experiments with a variety of oligosaccharides and polysaccharides are required to select favorable carbon sources for *T. eurrhizus*.

Acknowledgment

The author thanks to Professor Kazuhiko Kinjo, University of the Ryukyu for providing local strains of *Termitomyces*.

ABSTRACTS (MASTER THESIS)

Acceleration Mechanism of Radiation Belt Electrons by Whistler-mode Chorus Emissions

(Graduate School of Engineering, Laboratory of Computer Simulation for Humanospheric Sciences, RISH, Kyoto University)

Yu MIYASHITA

We analyze the mechanism of acceleration of energetic electrons interacting with whistler-mode waves in the Earth's radiation belts by using test particle simulations. First, in order to assess influence of the propagation angle of the whistler-mode wave on electron accelerations, we perform the test particle simulation in a simple model. By using the dispersion relation which is obtained from Maxwell's equations, we reproduce the electric field and the magnetic field of oblique whistler-mode waves. Then we set the electrons in the simulation field, we calculate the energy change of trajectory of electrons. In the simple model, we find that the larger propagation angle makes the effect of Landau resonance stronger. We then perform large-scale test particle simulations with chorus emissions for a prolonged time. By taking into account the adiabatic variation of the energetic particle distribution, we determine the resonant current. Then by solving general wave equations numerically, we obtain the time evolutions of the chorus wave frequency and amplitude along the Earth's dipole magnetic field. We simulate dynamics of electrons at the electron cyclotron scale by using the Buneman-Boris method. Following interactions with chorus emissions, we calculate a distribution function which corresponds to a Green's function for the chorus interaction. By repeating this process at different kinetic energies and pitch angles, we thereby obtain an electron distribution function after multi-cycle chorus emissions. The simulation results suggest that radiation belt electrons have been accelerated effectively by multi-cycle chorus emissions. Electrons which have energies less than 1 MeV have been accelerated strongly by the RTA process. On the other hand, electrons more than 1 MeV energies have been accelerated strongly by the URA process.

ABSTRACTS (MASTER THESIS)

Study on Microwave Power Beam Forming Methods with Panel Position Estimation for Panel-Structure Solar Power Satellite/Station

**(Graduate School of Engineering,
Laboratory of Applied Radio Engineering for Humanosphere, RISH, Kyoto University)**

Takaki Ishikawa

Introduction

A SPS (Solar Power Satellite/Station) is a gigantic satellite designed as an electric power plat orbiting in the GEO (Geostationary Earth Orbit) [1]. The SPS generates electricity from solar cell panels in space and transmits the electricity to a receiving site on the Earth by using a MPT (microwave power transmission) technology. In Japan, a tethered-SPS was proposed [2]. An image of the tethered-SPS is shown in Figure 1. We call a main unit of the tethered-SPS as a panel-structure SPS. The panel-structure SPS consist of a large number of power generation/transmission panel modules. This type of SPS is suitable for mass production and easy to maintenance. However, joints of the panel modules are flexible and the panel-structure SPS is difficult to maintain flatness of the transmission antenna surface. In order to achieve the high beam direction control accuracy, we have to correct the output phase errors caused by the antenna surface distortion. In this study, we describe one of the proposed beam correction methods which is called a PAC (Position and Angle Collection) method.

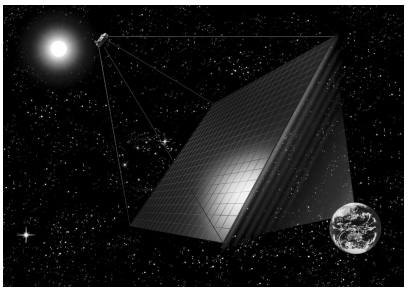

Figure 1. Image of a tethered-SPS [2]

Simulation of the PAC method

The PAC method is one of the beam correction methods for the panel-structure SPS. In the PAC method, we measure phases of a pilot signal, which was sent from a power receiving site on the Earth, on every panel module. We estimate the panel module positions by using the measurement phases. Then, considering the panel module positions, we correct the output phases of pilot signal. In this study, we simulated the PAC method by a 1D array model shown in Figure 2. Taking account of the SPS system, we set these parameters. At first, we simulated the accuracy of the PAC method. From the simulations, the pilot signal measurement points have to be put on the both ends of each panel module in order to achieve the high beam direction control accuracy. However, the spacing of two measurement points is much longer than the half wavelength of the pilot signal and ambiguities occur in the panel position estimation method. Because of the ambiguities, we can correct the output phase errors only when the panel module gradients are in the range of -5 degrees to 5 degrees. Thus, we propose an improved panel position estimation method. By using this estimation method, we can use the PAC method even if the panel module gradients are in the range from -50 degrees to 50 degrees.

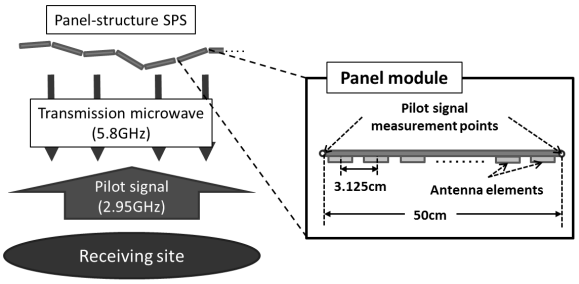

Figure 2. Schematic diagram of a 1D array model.

References

[1] P.E. Glaser, “Power from the Sun ; Its Future”, *Science*, No.162, pp.857-886, 1968.

[2] S. Sasaki, K. Tanaka, K. Higuchi, N. Okuizumi, S. Kawasaki, N. Shinohara, K. Senda, and K. Ishimura, “A New Concept of Solar Power Satellite : Tethered-SPS,” *Acta Astronautica*, Vol.60, pp. 153-165, 2006.

ABSTRACTS (MASTER THESIS)

Thrust Evaluation of Magnetic Sail by Using Plasma Particle Simulation

**(Graduate School of Engineering,
Laboratory of Space Systems and Astronautics, RISH, Kyoto University)**

Yasumasa Ashida

Magnetic sail is spacecraft propulsion that produces an artificial magnetosphere to block solar wind particles, and thus impart momentum to accelerate a spacecraft. In the present study, we conducted full particle-in-cell simulations on small-scale magnetospheres (Electron inertial scale) and Flux-Tube simulation on large-scale magnetospheres (Ion inertial scale) to investigate thrust characteristics of magnetic sail and its derivative, Magneto Plasma Sail (MPS), in which the magnetosphere is inflated by an additional plasma injection.

First, the simulations with the various magnetospheric sizes were performed to obtain the thrust level of the each magnetic sail. In Electron inertial scale, the Full-PIC simulation that treats both ions and electrons as particles is performed since the electron's finite Larmor radius effect and the charge separation between ion and electron become significant. In Ion inertial scale, the Flux-Tube model is performed, which neglects wave propagation and solves only a steady state of a plasma flow including the ion's finite Larmor effect. Therefore, the Flux-Tube model is expected to quickly estimate a thrust level with the low capacity of the computational memory. However, the Flux-Tube models developed for hall thrusters and ion engine grid do not include the effect of induced magnetic field. In the case of magnetic sail, the induced magnetic field has to be considered. Therefore, we constructed a new Flux-Tube model including the induced magnetic field [1]. As a result, the experimental formula for the thrust estimation is obtained and the thrust level from Electron scale to MHD scale is revealed. It is also shown that the MPS demonstrator spacecraft (L~500 m) can obtain the larger thrust by the magnetosphere inflation since the drag coefficient rapidly becomes larger in the scale.

In addition, the simulation for MPS was performed and the increase of the thrust was analyzed. We revealed that the plasma injection on the condition that the kinetic energy of plasma is smaller than the local magnetic field energy ($\beta \sim 10^{-3}$) can significantly inflate the magnetosphere by inducing diamagnetic current in the same direction as the onboard coil current. As a result, the MPS thrust is increased effectively by an additional plasma injection: the MPS thrust (15 μN/m) becomes up to 7.5 times larger than the original thrust of the magnetic sail (2.0 μN/m). In addition, we found that the thrust gain of MPS defined as "MPS thrust / Magnetic sail thrust + plasma injection thrust" becomes up to 2.2 [2].

As a result, the thrust of the magnetic sail from Electron inertial scale to Ion inertial scale and the attitude stability were revealed. These enable us to design the orbit of the magnetic sail supposing deep space missions. In addition, MPS with thermal plasma injection in 2D achieved to generate the high efficient thrust.

References

[1] Ashida, Y., Funaki, I., Yamakawa, H., Kajimura, Y. and Kojima, H., "Thrust Evaluation of a Magnetic Sail by Flux-Tube Model," Journal of Propulsion and Power, Vol. 28, No. 3, 2012, pp. 642-651.

[2] Ashida, Y., Funaki, I., Yamakawa, H. and Kajimura, Y., "Two-Dimensional Particle-In-Cell Simulation of Magnetic Sails," 32nd International Electric Propulsion Conference, Wiesbaden, Germany, September, 2011.

ABSTRACTS (MASTER THESIS)

Attitude dynamics of a charged satellite by Lorentz and gravity forces

**(Graduate School of Engineering,
Laboratory of Space Systems and Astronautics, RISH, Kyoto University)**

Shinji Hachiyama

A satellite naturally becomes charged in space filled with collisionless plasma. The relaxation methods for charging have been studied for a long time. Charged satellites are subjected to Coulomb forces from other charged satellites. Besides, the charged satellite is subjected to Lorentz force from the Earth's magnetic field. Control of charging a satellite is a good method to control orbit and attitude of satellites since it has the potential to lead novel dynamics. In the present thesis, we analyze the attitude motion of electrical-charged satellites using Lorentz force caused by Earth's magnetic field. Attitude control methods using gravity gradient torque are conventionally applied to a number of satellites. However, we apply them for the mission keeping and changing the attitude to the orbital radius direction. The objective is to demonstrate the attitude dynamics with the Lorentz force and the gravity force for the attitude control using these forces. The Earth's magnetic field is assumed to be dipole approximately. We numerically and analytically demonstrate the attitude dynamics using the formulated equation of motion. We found that the amount of charge in the equation is important for stability and instability of the attitude motion. Furthermore, the equilibrium points change depending on the quantity. On the basis of such property, we investigate methods to control the attitude of the satellite by controlling the amount of the charging. For example, Lorentz force makes the attitude stable to the directions except for the orbital radius direction and sustain the attitude of a charged satellite by controlling the amount of the charging. There are directions of the torque which cannot be generated by Lorentz force under the influence of the position and the attitude of the satellite. For that reason, we compared the amount of the torque in order to maintain the attitude by using only thrusters with by using additional Lorentz torque. With such comparison, we can evaluate the reduction ratio of the required torque.

References

[1] Yamakawa, H., S. Hachiyama, and M. Bando, “Attitude Dynamics of a Pendulum-shaped Charged Satellite,” IAA Acta Astronautica, Vol. 70, January-February 2012, pp. 77-84.

ABSTRACTS (MASTER THESIS)

Study on Integration of Analog Downconversion Circuits toward Small Plasma Wave Spectrum Receivers

(Graduate School of Engineering, Laboratory of Space Systems and Astronautics, RISH, Kyoto University)

Satoshi Okada

Space plasma is essentially collisionless, and its kinetic energy is transferred through plasma waves. Therefore, plasma waves reflect variations of electromagnetic environments in space. Plasma wave receivers, which capture the plasma waves, contribute to the investigations of the electromagnetic phenomena occurring in space. Sweep frequency analyzer (SFA), one of the types of the plasma wave receivers, provides spectral information of plasma waves with high frequency resolution and good signal-to-noise ratio. The plasma wave receivers, including SFA, are required to have low noise, high sensitivity, and wide dynamic range in wide band. These requirements lead analog circuits in the receiver to be large and heavy. Then, it difficult to realize small and lightweight receivers with discrete devices and commercial integrated circuits. We use ASIC (Application Specific Integrated Circuit) technology to downsize the analog part of the SFA. The objectives of the present thesis are to investigate the problem in development of the SFA downconversion circuits with ASIC technology, and to obtain perceptions to complete integration of the SFA into one chip. We design high gain main amplifier, mixer, and image rejecting Band Pass Filter (BPF) for the SFA. Each performance of the circuits is checked by simulations and trial productions of ASICs. First, the high gain amplifier is designed. 40 dB of the gain is confirmed by trial chips. Second, the mixer is designed. The gilbert cell is applied to the mixer. The linearity and inter-modulation distortions are evaluated. Third, the BPF is designed and evaluated with the trial chips. The BPF requires rapid reduction response, and high accuracy for manufacturing. The switched capacitor filter is employed to realize the BPF. Since the layout design is very important for the development of switched capacitor BPF, we discuss variations of frequency responses caused by parasitic capacitors and measures to reduce the effects. Finally, we examine expected characteristics of the analog downconversion system to be obtained by combining the designed mixer and the BPF. We also discuss how to enhance the performance as the analog downconversion system.

References

[1] Fukuhara, H., H. Kojima, S. Okada, H. Ikeda,H. Yamakawa, Temperature Compensated Gm ?C Filter for Plasma Wave Receivers Onboard Scienti?c Spacecraft, IEICE,Vol.J94-C, No. 6, pp. 155-162, 2011.(in Japanese)